

# Wind Sensors

## 9. Wind Sensors

Thomas Foken , Jens Bange 

Various techniques are used to measure the wind speed in the atmosphere, including cup, propeller, and sonic anemometers; the latter can also be used to measure the wind vector. Wind direction measurements are also performed using wind vanes. Sonic anemometers are the devices most commonly used for turbulence measurements. Hot-wire anemometers are employed for special measurements, and Pitot tubes are utilized for aircraft-based measurements. It is also important to note that the conditions at the measuring site can strongly influence the accuracy of wind measurements.

This chapter discusses the variables measured by all of the above devices as well as the corresponding measurement principles and their theoretical foundations. The technical data that each technique provides is presented, the maintenance that must be carried out when using each technique is described, and relevant quality control and calibration methods are introduced. The history of the development of wind sensors is also briefly summarized, and some examples of the application of wind measurements are presented.

9.1	<b>Measurement Principles and Parameters</b> .....	244
9.1.1	Measured Parameters .....	244
9.1.2	Measurement Principles .....	244
9.1.3	Siting Considerations .....	245
9.2	<b>History</b> .....	245
9.2.1	Wind Vanes .....	245
9.2.2	Mechanical Anemometers .....	246
9.2.3	Sonic Anemometers .....	248
9.2.4	Pressure Tube Anemometers .....	249
9.3	<b>Theory</b> .....	249
9.3.1	Cup and Propeller Anemometers .....	249
9.3.2	Sonic Anemometers .....	251
9.3.3	Thermal Anemometers .....	252
9.3.4	Hot-Wire Anemometers .....	252
9.3.5	Laser Doppler Anemometers .....	252
9.3.6	Pitot-Static or Prandtl Tubes .....	253
9.3.7	Wind Vanes .....	253
9.3.8	Scalar and Vector Averaging .....	253
9.3.9	Influence of the Surrounding Area on Wind Measurements .....	254
9.4	<b>Devices and Systems</b> .....	257
9.4.1	Rotation Anemometers .....	257
9.4.2	Wind Vanes .....	257
9.4.3	Combinations of a Rotation Anemometer with a Wind Vane .....	258
9.4.4	Sonic Anemometers .....	258
9.4.5	Thermal Anemometers .....	261
9.4.6	Hot-Wire Anemometers .....	261
9.4.7	Laser Anemometers .....	261
9.4.8	Pitot-Static or Prandtl Tubes .....	262
9.4.9	Comparison of Different Methods .....	262
9.5	<b>Specifications</b> .....	262
9.6	<b>Quality Control</b> .....	263
9.6.1	Wind Tunnel Calibration .....	263
9.6.2	Zero-Wind Chamber Calibration of Sonic Anemometers .....	265
9.6.3	Specific Quality Control Methods .....	265
9.7	<b>Maintenance</b> .....	266
9.8	<b>Application</b> .....	267
9.8.1	Climatology of Wind Parameters .....	267
9.8.2	Geostrophic Wind: Daily and Annual Cycles .....	267
9.8.3	Gusts .....	269
9.9	<b>Future Developments</b> .....	269
9.10	<b>Further Reading</b> .....	270
	<b>References</b> .....	270

The airflow in the atmosphere—the wind field—is crucial to the transport of air masses caused by the pressure field. Wind measurements are therefore necessary at all levels of the atmosphere to support weather forecasting

and to improve our understanding of global circulation and climate systems (see Chap. 1). Furthermore, fluctuations in the wind velocity (mainly its vertical component) are responsible for fluxes of momentum, heat, and

matter. The wind essentially determines the dispersion, transport, residence times, and changes in the mixing and concentrations of gases and particles. The high vari-

ability and significant vertical gradients in the wind field as well as the effects of heterogeneous landscapes on this field make measuring the wind a challenging task.

## 9.1 Measurement Principles and Parameters

The wind velocity is a vector with three components. For nonturbulent problems, usually only the horizontal wind speed and the direction of the mean wind are relevant, which are measured with separate sensors. This increases the number of wind parameters measured and sensor principles employed.

### 9.1.1 Measured Parameters

For the wind vector  $\mathbf{u}$ , it is assumed that

$$\mathbf{u} = f(U, \alpha), \quad (9.1)$$

where  $U$  is the magnitude (modulus) of the wind vector and  $\alpha$  is the direction of the wind vector from north via east. For the horizontal wind components  $u$  (east–west direction) and  $v$  (north–south direction), it follows that

$$u = U \sin \alpha \quad (9.2)$$

$$v = U \cos \alpha, \quad (9.3)$$

and the vertical wind component

$$w = U \sin \beta, \quad (9.4)$$

where  $\beta$  is the inclination of the wind field.

The fluctuations in the components

$$\begin{aligned} u &= \bar{u} + u' \\ v &= \bar{v} + v' \\ w &= \bar{w} + w' \end{aligned} \quad (9.5)$$

describe the turbulence (from Reynolds decomposition) [9.1]. Here, an overbar indicates an average and a prime symbol indicates a fluctuation. Typical averaging periods range from 10 to 30 min, with 10 min being a particularly common averaging period for operational wind observations. The sampling rate required to get an adequate description of the turbulent part is typically  $\geq 10$  Hz. The parameters that are measured are listed in Table 9.1. In the SI system (see Chap. 5), speeds are measured in meters per second ( $\text{m s}^{-1}$ ). However, other units are also used for speed in some Anglo-American countries and in particular fields, for example in aviation and in nautical applications (Table 9.2).

### 9.1.2 Measurement Principles

Many of the various techniques used to measure wind speeds were devised centuries ago, but anemometers based on them are still available commercially today and have their own fields of application. However, one of the more recently invented devices, the sonic anemometer, is becoming increasingly dominant (see Sect. 9.9) due to its ability to measure not just the mean wind speed but the whole three-dimensional wind vector (and therefore the wind direction). It is also able to measure the wind velocity with high resolution at frequencies of several tenths of a Hz. Instruments that can also be applied for turbulence measurements, such as hot-wire or laser anemometers, are less useful for performing measurements in the atmosphere and are therefore used mainly for calibration purposes. An overview of the various wind measurement principles is given in Table 9.3.

**Table 9.1** Parameters measured by wind sensors

Parameter	Description	Unit	Symbol
Windway	Distance that an air parcel covers within a certain time interval (older instruments)	m	
Wind speed	Horizontal wind velocity (mean value of both horizontal components)	$\text{m s}^{-1}$	$u_h$
Wind gust	A burst of high-velocity wind	$\text{m s}^{-1}$	$g_u$
Wind components, see (9.2)–(9.4)	Components of the wind vector in the Cartesian coordinate system: $u$ , $v$ are the horizontal components and $w$ is the vertical component	$\text{m s}^{-1}$	$u$ , $v$ , $w$
Fluctuations in the wind components	Fluctuations in the components of the wind vector in the Cartesian coordinate system: $u'$ , $v'$ are the horizontal components and $w'$ is the vertical component	$\text{m s}^{-1}$	$u'$ , $v'$ , $w'$
Wind direction	Direction that the wind comes from	°	

**Table 9.2** Units of wind speed

Unit	Transformation	Application
Beaufort	See Chap. 22	Nautical applications, partly in weather forecasting
Meter per second ( $\text{m s}^{-1}$ )	$1 \text{ m s}^{-1} = 2.236 \text{ mph} = 3.6 \text{ km h}^{-1}$	Widely used in meteorology and science
Kilometer per hour ( $\text{km h}^{-1}$ )	$1 \text{ km h}^{-1} = 0.62 \text{ mph} = 0.278 \text{ m s}^{-1}$	Traffic, partly in weather forecasting
Mile per hour (mph)	$1 \text{ mph} = 1.609334 \text{ km h}^{-1} = 0.44704 \text{ m s}^{-1}$	Meteorology (in some countries)
Knot (kn)	$1 \text{ kn} = 1.852 \text{ km h}^{-1} = 0.514 \text{ m s}^{-1}$	Nautical applications

**Table 9.3** Wind measurement techniques and their applicability to mean wind speed or turbulence measurements according to (9.5) [9.2]

Measuring device	Properties used to measure the wind				Applicability	
	Mechanical	Thermodynamic	Sound	Other	Mean	Turbulence
Cup anemometer	x				x	
Propeller anemometer	x				x	(x)
Thermal anemometer		x			x	
Hot-wire anemometer		x			x	x
Sonic anemometer			x		x	x
Laser anemometer				x	x	x
Pitot tube				x	x	x

### 9.1.3 Siting Considerations

Wind measurements can be strongly influenced by the measurement site. To obtain a representative wind field for a large region, the surroundings of the measurement site should be flat and free of obstacles; if this is not the case, the influence of the obstacles must be taken into account (see Sect. 9.3.9). These requirements are very important for measurements of the vertical gradient of the wind speed near the ground (see Chap. 54). Furthermore, when instruments such as cup anemometers and wind vanes are positioned relatively close, they should not disturb each other (ideally, the cup anemometer should be positioned about 0.1 m above the vane, and

the two instruments should be separated by about 1 m horizontally [9.3]).

According to the international guidelines [9.4], the standard measuring height in obstacle-free terrain is 10 m above the ground. The distance to the nearest obstacle should be ten times the obstacle height. In any case, the instrument must be installed 6–10 m above the mean height of buildings or the height of the surrounding vegetation.

Lightning strikes and other electric discharges pose a risk to wind-measuring instruments, as they can interfere with the measurements or destroy the equipment. The presence of lightning conductors can only remedy this situation to a limited extent.

## 9.2 History

The wind has been observed since ancient times; indeed, both Homer and the Bible speak poetically of four winds [9.5]. It is also known that the *Tower of Winds* in Athens (50 BCE) had an eight-point wind rose. During the Greek and Roman periods and right up to the sixteenth century in Italy, the wind direction was categorized into twelve winds: four groups of three centered on the four principal directions. The initials N, NNE, NE, ... were first used on a compass card in 1536 [9.6]. In addition, the history of wind measurements goes back about 2000 years.

### 9.2.1 Wind Vanes

Wind vanes have been in use since ancient times; for instance, the Tower of Winds had a wind vane. Wind vanes in the shapes of animals (such as snakes and dragons) or flags of kings were often used. Vanes in the shape of a rooster have been used on Christian churches ever since *Pope Nicholas I* (pontificate: 858–867) decreed that all churches must display this bird as an emblem [9.8]. The history of scientific instruments for measuring the wind started when the wind vane was

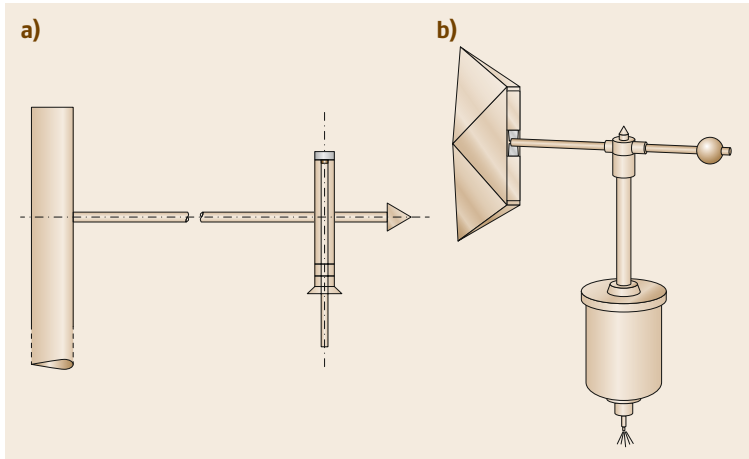


**Fig. 9.1a,b** Typical types of wind vanes: (a) the English R.A.E. pattern vane, (b) the German vane produced by Fuess (after [9.7], reproduced with permission from Springer, Berlin)

combined with a hand to show (and, later on, to register) the wind direction. In Florence in 1578, *Egnatio Danti* (1536–1586), a professor of mathematics at Bologna, built a wind vane with a single hand on a vertical dial, which was positioned on a 17 m high tower to ensure that wind measurements were not influenced by surrounding buildings [9.9]. A significant improvement in wind vane design was made by *Georges-Frédéric Parrot* (1767–1852) [9.6], the first rector of the Imperial University of Dorpat (now Tartu, Estonia). His design—a splayed vane—was a combination of two plates that diverged from the axis of the vane. His vane was relatively small; it was only about 19 cm in length and had a counterweight that was 11 cm long. This type of vane was used up to the twentieth century. However, in 1918, *Sir Geoffrey Ingram Taylor* (1886–1975) proposed a vane with an airfoil profile that became known in England as the *R.A.E. pattern vane* [9.10]. This vane precisely measures wind direction fluctuations with periods larger than 5 s [9.7]. In Germany, the wind vane produced by Fuess became popular (Fig. 9.1).

In 1788, *Franz Carl Achard* (1753–1821) developed an inclined wind vane to measure the vertical orientation of the wind field [9.6]. This system was used by micrometeorologists in combination with a propeller anemometer to measure the vertical wind velocity right up to the second half of the twentieth century, before sonic anemometers became available.

Weather vanes have long been employed to determine the wind direction; more recently, they have also been used in combination with anemometers [9.6]. Such vanes were included in the first meteographs (weather clocks, combinations of several instruments, including clocks), such as those constructed by *Robert Hooke* (1635–1703) in about 1678 and *Sir Christopher Wren* (1632–1723) in 1689. In 1789, the pastor *Christian Gotthold Herrmann* (1730–1792) of Cämmerswal-

de in Saxony constructed a machine with a twelve-point wind rose [9.11]. In this machine, a wheel was rotated by a wind vane carrying twelve radial compartments, and a hammer ejected a numbered cube from a magazine into the appropriate compartment of the relevant wind direction once every hour.

A professor of experimental physics in Milan, *Marsilio Landriani* (1751–1815), constructed a wind vane with eight pencils that marked the wind direction on a horizontal plate rotated by a clock. The professor of mathematics *James Henry Coffin* (1806–1873) at Easton (PA, USA) constructed a sand wind vane that used the same principle as Herrmann's instrument and distributed sand into 32 reservoirs. This instrument is currently being exhibited in the Museum of History and Technology in Washington, DC. In 1850, *Karl Kreil* (1789–1862), director of the observatory at Prague and the first director of the *Central Meteorological and Magnetic Bureau* at Vienna (from 1851), constructed another a wind vane using a pencil [9.12]. Several other instruments, including electrical recorders, have been constructed since then.

## 9.2.2 Mechanical Anemometers

Mechanical anemometers, which use the dynamic pressure of the wind field (see Chap. 12), can be grouped into swinging plate anemometers and rotation anemometers, while the latter can be further categorized into propeller and cup anemometers.

### Swinging Plate Anemometers

Around 1450, the Italian humanist and scientist *Leon Battista Alberti* (1404–1472) constructed the first swinging plate anemometer, where a plate moves along a scale under the influence of dynamic pressure (Fig. 9.2). Later, *Leonardo da Vinci* (1452–1519)

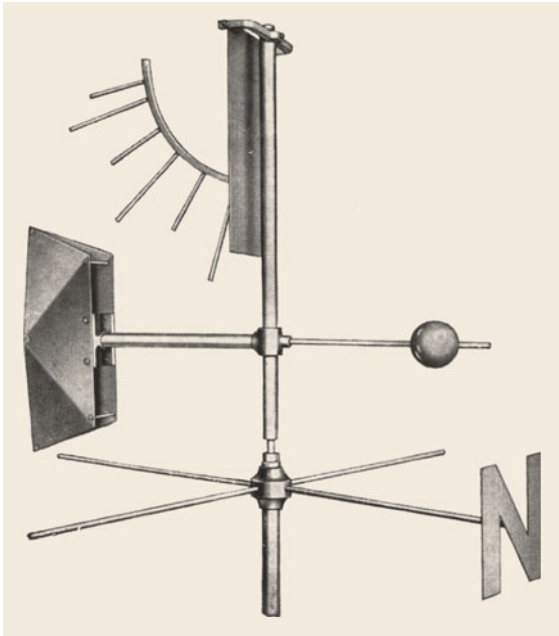


**Fig. 9.2** Swinging plate anemometer (*upper part*) made by von Wild (reprinted with permission from Dr. Alfred Müller, Meteorologische Instrumente KG, R. Fuess, Königs Wusterhausen, Germany)

painted the design of an instrument that looked similar to the one made by *Robert Hooke* (1635–1703) in 1684. Hooke’s construction—which was used by the Swiss meteorologist *Heinrich von Wild* (1833–1902), who was also the director of the St. Petersburg Observatory—can still be found in some stations and is available commercially (Fig. 9.2). Several more constructions, some of which form parts of more complex meteographs, are illustrated in [9.6].

#### Rotation Anemometers

The principle of a rotation anemometer is similar to that used by windmills, which have been employed in Europe since the twelfth century. Around 1678, *Robert Hooke* used this system for his weather clock. This principle was also used by the famous Russian scientist *Mikhail Vasilyevich Lomonosov* (1711–1765) for his anemometer, but he replaced the windmill with an overshoot water wheel [9.6]. In the first half of the nineteenth century, it was discovered that the rotation speed of this type of anemometer is dependent on the wind direction. This problem was overcome by combining the propeller with a wind vane (see Sect. 9.4.3) or through the precise application of the cosine dependency (see Sect. 9.4.1) of a propeller in helicoidal form. The first helicoid anemometer was built by the British meteorologist *William Henry Dines* (1855–1927) [9.13].



**Fig. 9.3** Robinson’s cup anemometer from 1846 [9.15] (courtesy of the NOAA Photo Library, National Oceanic and Atmospheric Administration, Department of Commerce)

The earliest known windmills with a vertical axis occurred in Persia in the seventh century CE; such windmills were not used in Europe, except in Poland. Those anemometers looked like present-day wind power generators with a vertical axis. The most famous vertical-axis windmill was built in 1734 by the postmaster of Louis XIV, *Louis-Léon Pajot, comte d’Ons-en-Bray* (1678–1754), and can be viewed in the exhibition of the Conservatoire National des Arts et Métiers in Paris. A similar device was built by the English scientist *William Whewell* (1794–1866) in 1838 [9.6].

Anemometers similar to the cup anemometer have probably been available since the end of the eighteenth century, as reported by the physician *Georg Wilhelm Munke* (1772–1747). The first cup anemometer dates back to 1846 and was constructed by the Irish astronomer *Thomas Romney Robinson* (1792–1882) [9.6, 14] (see Fig. 9.3), who modified Whewell’s anemometer and postulated a theory for the forces on the sensor. He got the idea for this novel design from the writer and engineer *Richard Lowell Edgeworth* (1744–1817), who constructed a windmill with a counter in 1793.

There is a long list of instruments that combine a wind vane with a rotation anemometer and a registration method [9.6, 7]. A modified version of one such instrument developed in the factory of R. Fuess in Berlin (*Heinrich Ludwig Rudolf Fuess*, 1838–1917) at the end

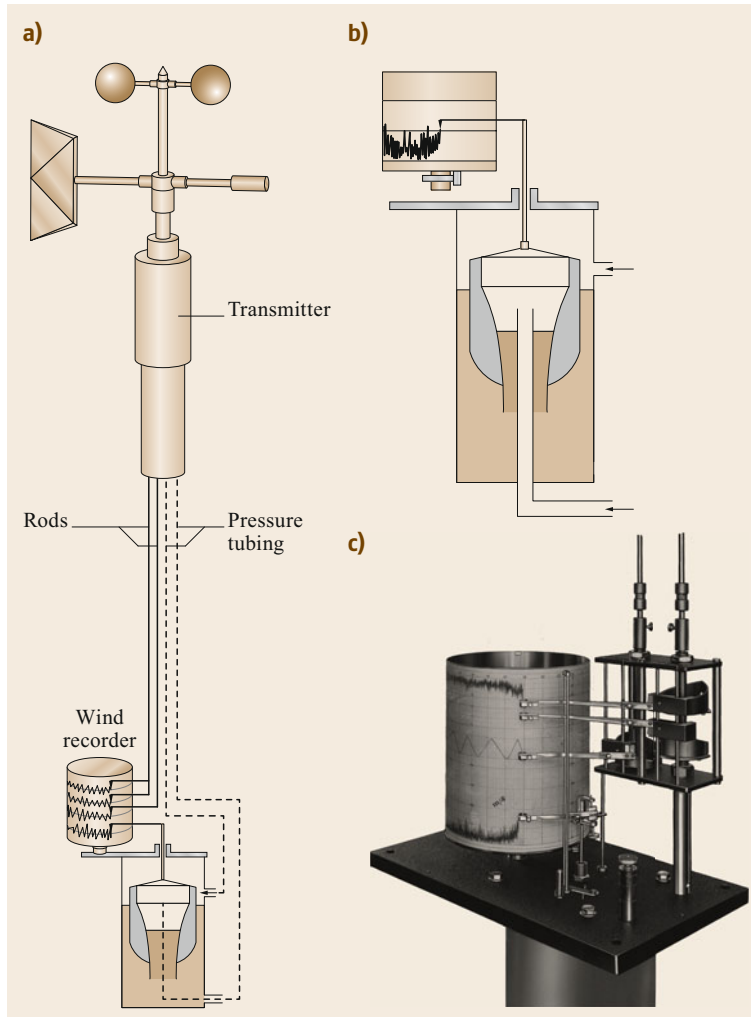


**Fig. 9.4a–c** Wind registration system invented by R. Fuess: **(a)** schematic view, **(b)** gust recorder, and **(c)** wind recorder unit (*upper part*: wind direction separated into N-E-S and S-W-N, *middle*: windway, *lower part*: gusts). Reprinted with permission from Dr. Alfred Müller, Meteorologische Instrumente KG, R. Fuess, Königs Wusterhausen, Germany

of the nineteenth century was used right up to the second half of the twentieth century, and is still commercially available. It combines a wind vane with a cup anemometer, measures the wind speed as the windway, and uses a Pitot tube (see Sect. 9.2.4) combined with a hydraulic system to measure gusts (this was termed a pressure-tube anemometer by *William Henry Dines* (1855–1927) in 1892 [9.6]; see Sect. 9.2.4 and Fig. 9.4).

### 9.2.3 Sonic Anemometers

The development of the eddy covariance method (see Chap. 55) required anemometers that responded rapidly. The basic equations for such anemometers were published in 1955 [9.16]. Following the development of the first sonic thermometer [9.17], a vertical sonic anemometer with a path length of 1 m was developed by *Verner Edward Suomi* (1915–1995) [9.18] and was used during the O’Neill experiment in 1953 [9.19]. Mod-

ern sonic anemometer designs are based on a system developed in 1960 by *Viktor Markovich Bovscheverov* (1905–1995) [9.20], which used the phase shift between sonic signals transmitted in different directions to calculate the wind vector. Subsequently, *Jagdish Chandran Kaimal* (1930–2021) and *Jost A. Businger* [9.21] (in 1963) and *Y. Mitsuta* [9.22] (in 1966) used the travel time of the sound in two directions to determine the velocity. The anemometer design used by the latter (Fig. 9.18a) is still employed today. Another sensor design that is still in use is the K-probe [9.23], so named because the sensor configuration is K-shaped.

However, the wind velocity measured using these instruments is temperature and humidity dependent. An approach that provided velocity measurements which were not subject to those influences was first realized in 1982 by *T. Hanafusa et al.* [9.27], who calculated the velocity components from the reciprocal travel times. This has become the dominant method in use



**Table 9.4** Milestones in sonic anemometer development (for further details, see [9.30])

Type of sonic anemometer	Institution	Year and reference
Phase shift	Institute of Physics of the Atmosphere, Moscow, Russia	1960 [9.20], 1973 [9.24]
	School of Agriculture, University of Nottingham, Loughborough, UK	1979 [9.25]
Travel time	University of Washington, Seattle, WA, USA	1963 [9.21]
	Disaster Prevention Research Institute, Kyoto University, Kyoto, Japan	1966 [9.22]
	Commonwealth Scientific and Industrial Research Organisation (CSIRO), Canberra, Australia	1983 [9.26]
	National Oceanic and Atmospheric Administration, Earth System Research Laboratories (NOAA/ESRL) Wave Propagation Laboratory, Boulder, CO, USA	1990 [9.23]
Reciprocal travel time	Meteorological Research Institute, University of Kyoto, Kyoto, Japan	1982 [9.27]
	University of Washington, Seattle, WA, USA	1986 [9.28, 29]

today. To reduce flow distortion effects and increase the accuracy of the vertical wind component, *John C. Wyngaard* and coworkers [9.28, 29] developed the University of Washington anemometer design, which is now widely used (Fig. 9.18b) and forms the basis of all omnidirectional anemometers.

### 9.2.4 Pressure Tube Anemometers

In 1675, the Paris-based instrument maker *Hubin* was intrigued to hear that Hooke could measure the wind without seeing it. Therefore, developing an idea proposed by *Pierre Daniel Huet* (1630–1721), Bishop von Soissons, France, he built an instrument consisting of a mercury-

filled U-tube with one open limb that was oriented towards the wind. Under the influence of the wind, the mercury in the U-tube moved into the other limb; the distance moved by the mercury was dependent on the wind speed. Unfortunately, however, the measured signal was very small [9.6]. In 1732, this concept was used by the French engineer *Henri Pitot* (1695–1771) to measure water flow [9.31], and the instrument was modified into its present form—the so-called Pitot tube—by the French scientist *Henry Darcy* (1803–1858) [9.32] in the middle of the nineteenth century. In the 1890s, *William Henry Dines* (1855–1927) modified the instrument to measure gusts in a similar manner to the device built by R. Fuess in Berlin (see Sect. 9.2.2).

## 9.3 Theory

Mechanical anemometers and wind vanes are classic examples of first- and second-order dynamical systems. A general description of these systems is given in Chap. 2. In the following section, relevant characteristics of these instruments and other anemometers are listed together with factors that influence them and the theory behind these measurement principles.

### 9.3.1 Cup and Propeller Anemometers

Classical wind measuring devices such as cup and propeller anemometers (see Figs. 9.12 and 9.13) are based on a mechanical principle whereby the dynamic pressure of the airflow is transformed into rotational movement. The horizontal wind speed  $u$  can be calculated directly from the geometry of the cup anemometer when the drag coefficients  $C_D$  of the cups are known. According to Bernoulli's law (see Chap. 10), the force  $F$  on any fixed surface with an area  $A$  perpendicular to the wind is given by [9.33]

$$F = C_D A \frac{\rho}{2} u^2, \quad (9.6)$$

where  $\rho$  is the air density. Without any loss of generality, we can assume that the cup anemometer consists of only two cups. If there is no acceleration (i.e., assuming stationarity), the forces on both cups are the same. Now consider the instant that the lever arm connecting the cups is perpendicular to the flow. At this point, one cup exposes its convex (closed) side to the flow. This cup is moving towards the flow with a rotational speed  $u_{\text{rot}}$ . Its surface experiences a wind speed of  $u + u_{\text{rot}}$ . The other cup shows its concave (open) side to the flow and is moving away from it. The balance of forces is therefore

$$C_D^{\text{closed}} A \frac{\rho}{2} (u + u_{\text{rot}})^2 = C_D^{\text{open}} A \frac{\rho}{2} (u - u_{\text{rot}})^2. \quad (9.7)$$

This quadratic equation leads to two solutions, but only one is physically meaningful,

$$u = u_{\text{rot}} \frac{\sqrt{C_D^{\text{open}}} + \sqrt{C_D^{\text{closed}}}}{\sqrt{C_D^{\text{open}}} - \sqrt{C_D^{\text{closed}}}} > u_{\text{rot}}. \quad (9.8)$$

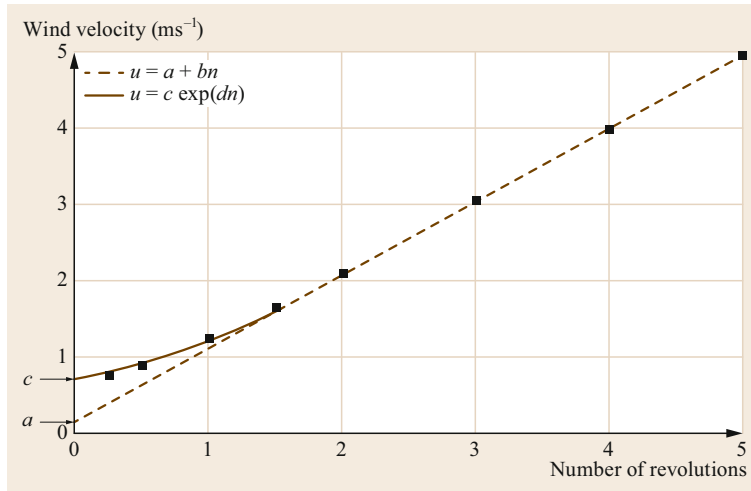


**Fig. 9.5** Transfer function of a cup anemometer;  $n$  is the number of revolutions of the anemometer,  $u$  is the wind speed, and  $a$ ,  $b$ ,  $c$ , and  $d$  are constants (after [9.3], reproduced with permission from VDI e.V., Düsseldorf, Germany)

For spherical cups,  $C_D^{\text{open}} \approx 1.33$  and  $C_D^{\text{closed}} \approx 0.33$  are good approximations.

In order to calibrate mechanical anemometers, it is very important to know the transfer function between the speed in a wind tunnel and the speed measured with the anemometer. This is the linear relationship between the wind speed and the rotation speed of the anemometer within a defined working range, which must be determined in a wind tunnel [9.34–36]. It takes the form

$$u = a + bn, \quad (9.9)$$

where  $u$  is the wind speed,  $n$  is the number of rotations,  $a$  is the extrapolation of the transfer function to zero revolutions, and  $b$  is a constant: the sensitivity of the instrument. This relationship is linear over a wide range of speeds, but at low speeds ( $< 2\text{--}4 \text{ m s}^{-1}$ ) it is necessary to use the exponential approximation

$$u = c \exp(dn) \quad (9.10)$$

because a rotating anemometer has a threshold speed  $c$  (about  $0.1\text{--}0.3 \text{ m s}^{-1}$ ), which is the lowest wind speed that causes the rotating anemometer to move continuously (this should not be confused with  $a$  in the linear transfer function). This is illustrated in Fig. 9.5.

The time constant (see Chap. 2) of a rotation anemometer depends on the wind velocity. Therefore, the velocity-independent distance constant [9.34–36]

$$L = u_\infty \tau, \quad (9.11)$$

where  $u_\infty$  is the final velocity and  $\tau$  is the time constant, is a measure of the inertia of the anemometer and gives the wind path (the passage of the air within a certain time interval or the exact product of wind

speed and time) required for an anemometer to register 63% of a wind speed difference. The distance constant is an important parameter of the inertia of mechanical anemometers; it is about 1 m for sensitive propeller anemometers, about 2–3 m for small cup anemometers, and about 5 m for larger anemometers. This constant should be used instead of the threshold speed to assess the measurement quality because the starting speed is generally below  $0.5\text{--}1.0 \text{ m s}^{-1}$ , and the turbulent wind field is not fully developed at these speeds. Low values for the response characteristics are required for gust measurements (see Sect. 9.8.3), where the usual averaging interval is 3 s and the sampling rate  $\leq 4 \text{ Hz}$  [9.4].

As the distance constant increases, overestimation of the wind speed starts to occur due to torque on the cup rotor (overspeeding [9.36]). This overestimation of the measured wind speed relative to the true wind speed is induced by turbulence. Wind gusts will cause a mechanical anemometer to rapidly rotate due to a high torque. However, after the gust, the anemometer will require some time to adjust to the moderate wind speeds. There is no compensation for these additional rotations when the wind speed is low. Overspeeding can be as large as 10% of the wind velocity and is particularly large for low wind speeds and high distance constants. The overspeeding is proportional to  $(\sigma_u/u)^2$ , where  $\sigma_u$  is the standard deviation of the wind speed ( $u$  is the horizontal wind speed here). If overspeeding in measurements near the ground is not accounted for, wind gradients will be inaccurate.

A cosine response cannot be assumed for cup anemometers. If there is only a moderate inclination of the flow, the measured wind speed will always be roughly the same. This means that cup anemometers overestimate the wind speed for an inclined flow [9.35].



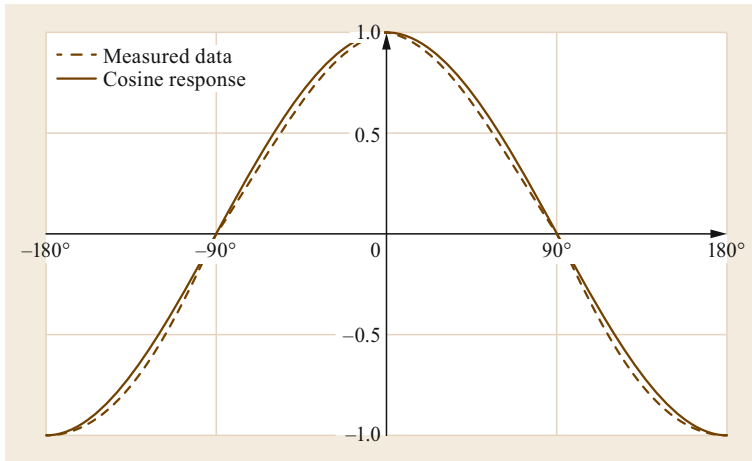


**Fig. 9.6** Cosine response of a propeller anemometer (after [9.2])

For propeller anemometers (see Sect. 9.4.1), the cosine response is defined as the ratio of the measured wind speed for a certain angle of incidence  $\alpha$  to the wind speed of the horizontal wind field  $u(\alpha = 0)$  multiplied by the cosine of the angle, i.e.,

$$F(\alpha) = \frac{u(\alpha)}{u(0) \cos \alpha}. \quad (9.12)$$

An ideal cosine response is  $F(\alpha) = 1$ . For propeller anemometers, deviations of up to 15% occur for incidence angles of about  $45^\circ$  (Fig. 9.6). For the light helicoidal propellers that tend to be used in three-dimensional propeller anemometers, these deviations can be relatively simply corrected using the relation

$$u_{\text{corr}}(\alpha) = u_{\text{meas}}(\alpha) [\cos \alpha - a \sin(2\alpha)], \quad (9.13)$$

where  $a = 0.085$  [9.37] or  $a = 0.140 - 0.009u$  [9.38]. For crosswinds ( $\pm 90^\circ$ , see Fig. 9.6), there is a dead zone of approximately  $\pm 2^\circ$  where the propeller does not rotate. In measurements of the vertical wind, the dead zone is eliminated by employing two inclined sensors. It is recommended that a shank extension should be used for flow from the front [9.39] so that the dynamic conditions of the propeller are nearly identical for flow from the front and flow from behind.

### 9.3.2 Sonic Anemometers

Modern sonic anemometers use the travel time principle and direct time determination [9.27]. In this method, a sonic signal (about 100 kHz) is transmitted from both sides of the measurement path and received on the opposite sides (Fig. 9.7). Due to the wind velocity, one signal is faster than the other. The wind velocity is de-

termined from the exact travel times of the sonic signals

$$t_{1,2} = \frac{\sqrt{c^2 - u_n^2} \pm u_d}{c^2 - u^2} d, \quad (9.14)$$

where  $d$  is the path length,  $u_d$  is the wind component along the path,  $u_n$  is the normal component of the wind, and  $c$  is the speed of sound. This relation is based on the assumption that the flow in the sonic anemometer is slightly shifted by an angle  $\gamma$  from the measurement path, and the travel times are given by [9.35, 40]

$$t_{1,2} = \frac{d}{c \cos \gamma \pm u_d}. \quad (9.15)$$

The difference in reciprocal travel times gives the wind velocity along the measurement path, i.e.,

$$\frac{1}{t_1} - \frac{1}{t_2} = \frac{2}{d} u_d, \quad (9.16)$$

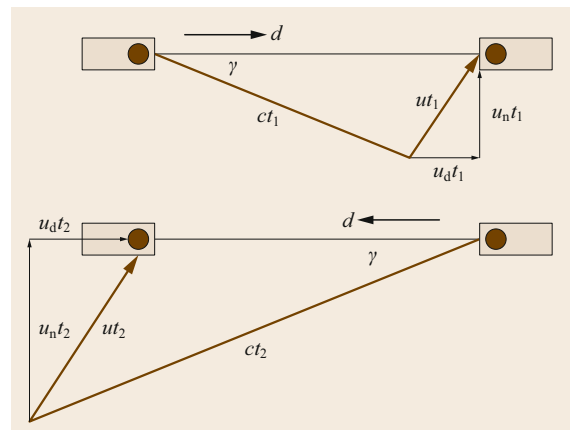


**Fig. 9.7** Vector graph of the sound paths of a sonic anemometer (after [9.2])

and the sum of the reciprocal travel times eliminates the speed of sound, from which the so-called sonic temperature can be calculated (see Chap. 7). This equation also gives the computational detection limit for the wind speed based on the resolution of the runtime measurement  $t_{1,2}$  and the error in the measuring path length. In practice, the detection limit is often given by the zero-point drift of the speed measurement, which can be verified in a null wind chamber [9.41] (see Sect. 9.6.2). The transducers and the mounting rods deform the wind field. These effects can be determined through wind tunnel calibrations. However, this shadow error is usually lower in the turbulent wind field. This is discussed in detail in Chap. 55.

### 9.3.3 Thermal Anemometers

Thermal anemometers use a protected cylinder at  $\Delta T = 50\text{ K}$  higher than the air temperature  $T$  as a measuring element. Temperature sensors are arranged over the cylinder's surface. The heater voltage  $U$  to keep the temperature difference constant in time at  $\Delta T = 50\text{ K}$  (using a loop control system) is used to measure the wind speed  $u$  via [9.3]

$$u = c_t \frac{T}{p} (U^2 - U_0^2)^2, \quad (9.17)$$

where  $c_t$  is a sensor-specific constant,  $p$  is the air pressure, and  $U_0$  is the reference voltage at  $u = 0\text{ m s}^{-1}$ . The wind direction is obtained from the measured temperature distribution on the cylinder's surface using a compensating curve.

### 9.3.4 Hot-Wire Anemometers

Depending on the measurement electronics employed, a hot-wire anemometer can be utilized as a constant-voltage anemometer (CVA), constant-current anemometer (CCA), or constant-temperature anemometer (CTA). The latter requires a constant electrical resistance  $R$  and is a very common instrument in atmospheric physics. A number of variables determine the voltage that is required to keep the resistance  $R(T)$  of the wire, and thus its temperature  $T$ , constant: the voltage  $U$  applied to the wire, the electrical current  $I$  through the wire, the Reynolds number  $Re$  of the flow across the wire (expressed by an exponent  $n \approx 2$  for most atmospheric flows, see below), the temperature difference  $T_{\text{wire}} - T_{\text{air}}$  between the wire and the ambient, the air density  $\rho$ , the heat capacity and conductivity of the wire (expressed by two material constants,  $c_1$  and  $c_2$ ), the heat  $H$  transferred from the wire to the ambient through convection, the heat radiated, by the wire and heat conducted from the wire to the mounting.

Above a certain wind speed  $u$ , the heat transfer  $H$  to the ambience is governed by forced convection, so radiation and heat conduction to the mounting can be neglected, implying that

$$H \approx [c_1 + c_2(\rho u)^{\frac{1}{n}}](T_{\text{wire}} - T_{\text{air}}). \quad (9.18)$$

This means that a CTA only works correctly for significant wind speed (typically above  $0.2\text{ m s}^{-1}$ ).

The heat  $Q$  stored in the wire changes over time  $t$  according to *King's law* of convective heat transfer,

$$\frac{dQ}{dt} = I^2 R - H = \frac{U^2}{R} - H, \quad (9.19)$$

after applying Ohm's law. In the quasi-stationary state  $dQ/dt = 0$ , the electrical heating equals the loss of  $H$ , and *King's law* becomes

$$U^2 = [c_1 + c_2(\rho u)^{\frac{1}{n}}](T_{\text{wire}} - T_{\text{air}})R(T_{\text{wire}}), \quad (9.20)$$

assuming the presence of a loop control circuit that keeps the wire temperature (and thus  $R$ ) constant and allows the voltage  $U$  to be measured. Of course, the air temperature  $T_{\text{air}}$  must also be measured, preferably using a similar method (a cold thin-wire resistance thermometer, see Chap. 7) that delivers highly resolved turbulent temperature data. For further details on hot-wire (and hot-film) anemometers, see [9.42]; for more on air density, please refer to Chap. 5.

### 9.3.5 Laser Doppler Anemometers

Laser Doppler anemometers tend to be applied more commonly in laboratories and wind tunnels than in the atmosphere, with its fluctuating aerosol concentration. Such anemometers usually employ two monochromatic light beams that cross at a small angle  $\phi$ . The beams generate a standing interference field, and the frequency of the fluctuations is equal to the Doppler shift between the incident and scattered light. The frequency  $f$  is proportional to the velocity component  $u_a$  parallel to the measurement axis [9.3] (see also Fig. 9.8) such that

$$f = \frac{|u_a|}{d_f}, \quad (9.21)$$

where  $d_f$  is the period of the interference field, which depends on the wavelength of the light and the angle  $\phi$ .

The simplest geometry involves the reflection of a single light beam of wavelength  $\lambda$  (and frequency  $f_{\text{laser}} = c/\lambda$ , where  $c$  is the speed of light) by an air particle moving along the direction of light propagation with a velocity component  $u$ . Due to the Doppler shift,

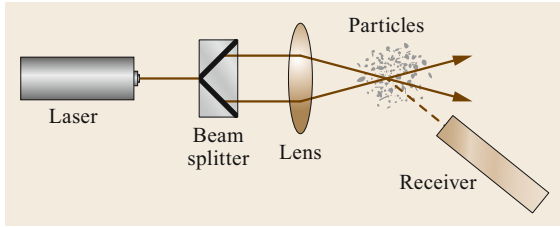


**Fig. 9.8** Schematic of a dual-beam laser Doppler anemometer

the reflected light (along the direction of light propagation) is shifted in frequency ( $f_{\text{scatter}}$ ) towards the blue when the particle is moving towards the photodetector and towards the red when the particle is moving away from the sensor. The velocity component  $u_a$  can be calculated using

$$u_a = \frac{\lambda}{2} (f_{\text{laser}} - f_{\text{scatter}}). \quad (9.22)$$

A two-beam geometry allows the measurement of the velocity component  $v$  perpendicular to the direction of propagation of the light. In this case, the laser beam is split into two beams with identical wavelengths that are focused at an angle  $\phi$ . A photodetector on the opposite side of the focus detects the two beams with different frequencies  $f_1$  and  $f_2$  due to the movement perpendicular to the beam axis. The corresponding velocity component of the scattering particle is

$$v = \frac{\lambda (f_2 - f_1)}{2 \sin \frac{\phi}{2}}. \quad (9.23)$$

Further details on laser Doppler anemometers (LDAs) can be found in [9.42, 43].

### 9.3.6 Pitot-Static or Prandtl Tubes

In order to measure the wind velocity norm  $u = |\mathbf{u}|$  using Bernoulli's equation (see Chap. 10) along with a Pitot-static tube (also known as a Prandtl tube) in combination with (for instance) a wind vane, it is necessary to measure the pressure  $p_{\text{stag}}$  at the stagnation point of the tube (i.e., the sum of the kinetic and potential energies of the flow) as well as the static air pressure  $p_s$ ; see Fig. 9.9. The wind velocity can then be calculated



**Fig. 9.9a–c** Schematics of various Pitot tube configurations: (a) simple Pitot tube (sum of the dynamic and static pressures), (b) static tube (static pressure only), and (c) Pitot-static tube (Prandtl tube)

using (10.9) (see Chap. 10) as the dynamic pressure enhancement, i.e.,

$$u = \sqrt{2 \frac{p_{\text{stag}} - p_s}{\rho}}. \quad (9.24)$$

### 9.3.7 Wind Vanes

The wind vane is the classical instrument for measuring the wind direction. It is a second-order dynamical system (see Chap. 2). A wind vane consists of a wind direction indicator that can rotate about a vertical axis. The wind produces a torque on the vane that is proportional to the square of the wind speed and turns the vane in the direction of the wind. Turbulence generates oscillations that over- and undershoot the true wind direction  $\phi_f$ . Wind vanes are designed to achieve a sufficiently short response time and high resolution. The damped natural wavelength is given by [9.3]

$$\lambda_d = Pu, \quad (9.25)$$

where  $P$  is the period of the damped oscillation. The undamped natural wavelength is

$$\lambda_n = \lambda_d \sqrt{1 - D^2}, \quad (9.26)$$

where  $D$  is the damping ratio, which should be between 0.3 and 0.7 [9.4] to limit any overshooting [9.44] and achieve a reasonable response time [9.45], and which is also given by a distance constant  $d$ , often for 50% of the change in wind direction (see Fig. 9.10). The damping ratio can be obtained from [9.35, 44, 46, 47]

$$D = \frac{1}{\sqrt{1 + \left[ \frac{\pi}{\ln(a_2/a_1)} \right]^2}}, \quad (9.27)$$

where  $a_1$  is the deviation of the wind vane and  $a_2$  is the amplitude of the first overshoot, as illustrated in Fig. 9.10.

### 9.3.8 Scalar and Vector Averaging

The typical averaging interval for wind data is 10 min, although an interval of 30 or 60 min is used in some applications. Due to the vectorial nature of the wind,

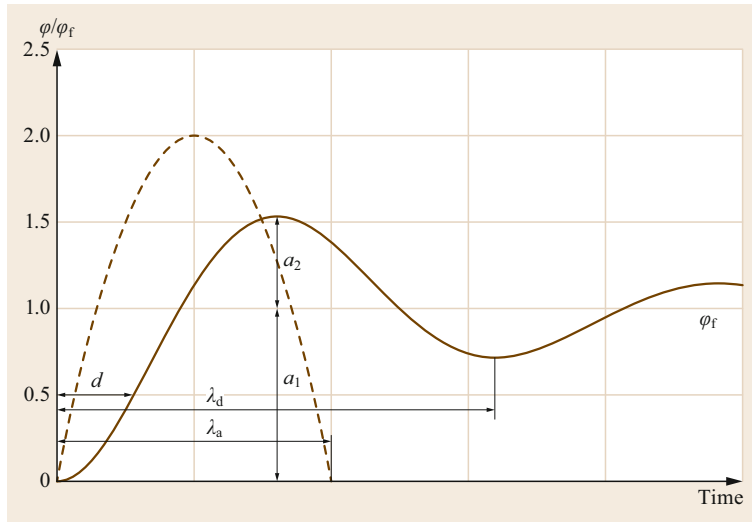


**Fig. 9.10** Plot showing the parameters involved in the damping of a wind vane

the averaging of wind data at a much greater temporal resolution than 10 min (e.g., 10 s) necessitates special calculations [9.3].

Averaging with time intervals of more than an hour is not meaningful; when the time intervals are large, probability density functions are calculated instead (see Sect. 9.8.1).

**Vector Averaging**

Vector averaging is the most physically precise of these calculations, although it assumes that the vertical wind component is zero during the averaging period for a horizontal wind field.

Direct averaging of the wind direction leads to systematic mistakes (e.g. averaging northern wind directions 350° and 1° would lead to 180°). Thus for the direction of the mean horizontal wind vector, both horizontal components *u* (9.2) and *v* (9.3) have to be averaged separately. The mean wind components from *N* individual values are defined as

$$\bar{u} = \frac{1}{N} \sum_{i=1}^N u_i \tag{9.28}$$

and

$$\bar{v} = \frac{1}{N} \sum_{i=1}^N v_i \tag{9.29}$$

The mean horizontal wind speed can be calculated from both components as

$$\bar{u}_h = \sqrt{\bar{u}^2 + \bar{v}^2} \tag{9.30}$$

**Table 9.5** Direction angle  $\bar{\alpha}$  as a function of the signs of the components *u* and *v* of the wind vector [9.3]

$\bar{u}$	$\geq 0$	$\geq 0$	$< 0$	$< 0$
$\bar{v}$	$> 0$	$< 0$	$< 0$	$> 0$
$\bar{\alpha}$	$\bar{\alpha}'$	$180^\circ - \bar{\alpha}'$	$180^\circ + \bar{\alpha}'$	$360^\circ - \bar{\alpha}'$

and the initial mean wind direction is

$$\bar{\alpha}' = \arctan \left| \frac{\bar{u}}{\bar{v}} \right|, \text{ where } 0^\circ \leq \bar{\alpha}' \leq 90^\circ \tag{9.31}$$

Note that *v* = 0 is not allowed in this equation. In this case,  $\bar{\alpha} = 90^\circ$  for *u* > 0 and  $\bar{\alpha} = 270^\circ$  for *u* < 0. The true mean direction angle  $\bar{\alpha}$  can be obtained from the signs of the components of the wind vector in accordance with Table 9.5.

**Scalar Averaging**

When the measurements obtained are scalar means (e.g., data from cup anemometers), the mean horizontal wind speed can be calculated as

$$\bar{u}_h = \frac{1}{N} \sum_{i=1}^N u_{hi} \tag{9.32}$$

Since the wind direction scale is discontinuous at north, if there are direction changes that take place via north, the scale must be extended beyond 360° when calculating the mean wind direction.

**9.3.9 Influence of the Surrounding Area on Wind Measurements**

Wind measurements are significantly influenced by buildings, trees, and other obstacles in the vicinity of

the measurement site. Several more or less phenomenological rules have been developed to aid the selection of measurement sites and the correction of measurements. Very expensive wind tunnel studies or large eddy simulations are needed to exactly determine the influences of nearby obstacles. The methods outlined below are recommended for standard wind measurements.

The World Meteorological Organization (WMO) has developed a clear schema for classifying and correcting wind measurements [9.4, 48]. The recommended height at which measurements should be performed is 10 m. Because not all sites have the ideal characteristics of being exactly flat and having low roughness and no obstacles, it is recommended that stations should be classified as shown in Table 9.6 (see also Chap. 43), and that terrains should be classified based on the roughness length (Table 9.7; see also Chap. 1).

It is generally difficult to correct wind measurements precisely. However, the following three methods can be used to correct wind measurements sufficiently to allow rough comparisons between data obtained at different locations. Note that the methods do not give precisely comparable results, and corrections should only be made if the site is not too rough ( $z_0 \leq 0.5$  m).

WMO has proposed a correction method for the station classification mentioned above [9.4, 48] that depends on the roughness length, a flow distortion cor-

rection [9.28, 52], and a topographic correction [9.53, 54]. For the corrected wind speed, it follows that

$$u_{\text{corr}} = u_{\text{meas}} C_F C_T \frac{\ln(10 \text{ m}/z_{0u})}{\ln(z/z_{0u})} \times \frac{\ln(60 \text{ m}/z_{0u}) \ln(10 \text{ m}/z_0)}{\ln(10 \text{ m}/z_{0u}) \ln(60 \text{ m}/z_0)}, \quad (9.33)$$

where  $z_0$  is the roughness length at the site,  $z_{0u}$  is the effective roughness length of the terrain upstream of the site,  $C_F$  is the flow distortion factor (which is 1 for a free-standing mast), and  $C_T$  is the topographic correction factor, which is the ratio of the regional average wind speed to the wind speed at the site (this ratio is 1 for flat terrain). The effective roughness length is a correction for roughness effects and obstacles up to 2 km upstream of the site. To determine the effective roughness length, the climatology (one year) of the standard deviation of the horizontal wind speed  $\sigma_{uh}$  and the standard deviation of the wind direction  $\sigma_d$  (in radians) for sectors of roughly  $30^\circ$  must be applied, i.e.,

$$\frac{\sigma_{uh}}{u} = c_u \kappa \left[ \ln \left( \frac{z_0}{z_{0u}} \right) \right]^{-1} \quad (9.34)$$

or

$$\frac{\sigma_d}{u} = c_v \kappa \left[ \ln \left( \frac{z_0}{z_{0u}} \right) \right]^{-1}, \quad (9.35)$$

**Table 9.6** Recommended classification of wind measurement sites (modified from [9.4, 48])

Class	Minimum distance to obstacles		Angular width (degrees)	Remark	Roughness class (see Table 9.7)	Uncertainty (correction required) (%)
	Surrounding obstacles	Thin obstacles more than 8 m high (masts, thin trees)				
1	> 30 times the height of obstacles	> 15 times the height of thin obstacles	$\leq 1.9$	Obstacles < 4 m high should be ignored	2–4	–
2	> 10 times the height of obstacles	> 15 times the height of thin obstacles	$\leq 5.7$	Obstacles < 4 m high should be ignored	2–5	$\leq 30$
3	> 5 times the height of obstacles	> 10 times the height of thin obstacles	$\leq 11.3$	Obstacles < 5 m high should be ignored		$\leq 50$
4	> 2.5 times the height of obstacles; no obstacles with an angular width > $60^\circ$ and a height > 10 m within 40 m		$\leq 21.8$	Obstacles < 5 m high should be ignored		> 50
5	Sites that do not meet the requirements of class 4 are not recommended for wind measurements					

**Table 9.7** Recommended terrain classification based on the roughness length  $z_0$  [9.4] (updated according to [9.2, 49, 50]);  $x$  is the fetch and  $H$  is the obstacle height

Class	Surface	Obstacles	Roughness length $z_0$ (m)
1	Open sea	$x \geq 5$ km	0.002
2	Flat bare soil, snow	No	0.005
3	Open flat terrain, grass	No	0.03
4	Low crops	Occasional obstacles $x/H > 20$	0.1
5	High crops	Scattered obstacles $15 < x/H < 20$	0.25
6	Parkland, bushes	Numerous obstacles $x/H \approx 10$	0.5
7	Suburb, forest	Regular large obstacles	1.0
8	City center	High- and low-rise buildings	2.0

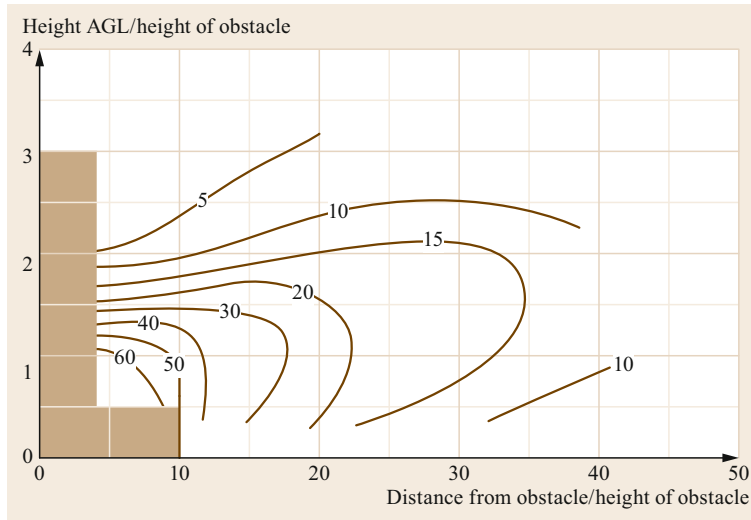


**Fig. 9.11** Determination of the factor  $R_1$  (after [9.51], reproduced with the permission of the Danish Technical University, Roskilde, Denmark)

where  $c_u = 2.2$ ,  $c_v = 1.9$  [9.2], and the *von Kármán* constant  $\kappa = 0.4$ .

A similar method was developed by the German Meteorological Service based on older versions of the WMO guidelines [9.4, 55]. This method is based on obstacle width ( $B$ ) and height ( $H$ ). For tall, narrow obstacles ( $H \gg B$ ), the distance  $A$  between the measuring instrument and the obstacle is

$$\begin{aligned} A &\geq 0.5H + 10B && \text{for } B \ll H \leq 10B \\ A &\geq 15B && \text{for } H > 10B. \end{aligned} \quad (9.36)$$

For  $H \approx B$ , it follows that

$$A \geq 5(H + B), \quad (9.37)$$

and for flat, elongated obstacles ( $H \ll B$ ),

$$\begin{aligned} A &\geq 0.5B + 10H && \text{for } H \ll B \leq 10H \\ A &\geq 15H && \text{for } B > 10H. \end{aligned} \quad (9.38)$$

When there are circular obstacles of radius  $r$  surrounding the installation site (e.g., the site is surrounded by houses or forest clearings), it follows that

$$\begin{aligned} A &\geq \pi r + 10H && \text{for } H \geq \frac{\pi}{5}r \\ A &\geq 15H && \text{for } H < \frac{\pi}{5}r. \end{aligned} \quad (9.39)$$

If the minimum distance  $A$  cannot be complied with (9.36)–(9.39), the wind speed will not be corrected, but the instrument's pole must be raised by  $h'$ , where

$$h' = \frac{H}{A} (A - A_D). \quad (9.40)$$

Here,  $A$  is the distance assessed using (9.38) to (9.41), and  $A_D$  is the distance between the obstacle and the actual measurement site.

The European Wind Atlas [9.51] applies a method based on [9.56] to determine the lee side of an obstacle. Accordingly, a corrected wind velocity can be calculated from the measured velocity and the porosity  $P$  of the obstacle (buildings:  $P = 0.0$ ; trees:  $P = 0.5$ ) as

$$u_{\text{corr}} = u_{\text{meas}} [1 - R_1 R_2 (1 - P)]. \quad (9.41)$$

The factor  $R_1$  can be obtained from Fig. 9.11, and

$$R_2 = \begin{cases} \left(1 + 0.2 \frac{A}{B}\right)^{-1} & \text{for } \frac{B}{A} \geq 0.3 \\ 2 \frac{B}{A} & \text{for } \frac{B}{A} < 0.3. \end{cases} \quad (9.42)$$

For measurements of turbulent fluxes (see Chap. 55), the recommended distances should be enlarged by a factor of 5–10. The footprint (see Chap. 1) should also be taken into account. Similar conditions must be fulfilled for measurements of the vertical gradients of the horizontal wind speed, which are sometimes gauged to determine the stratification conditions in the atmosphere or energy and substance exchanges (see Chaps. 54 and 57), and are usually performed at small heights ( $< 10$  m). For a discussion of the influence of the sensor installation (i.e., the tower), see Chap. 6. Special requirements may also call for the sensor to be installed at a greater or lower height than normal (e.g., at source height) or the measurement of locally relevant data (e.g., in street canyons).



## 9.4 Devices and Systems

Anemometers and wind vanes are available as individual instruments or they can be integrated into one system. Rotation anemometers and wind vanes are installed close together, while sonic and thermal anemometers that measure the wind speed and direction are usually integrated into one sensor. Hot-wire, laser, and Pitot anemometers are seldom applied in the atmosphere, but they are used for calibration in wind tunnels.

### 9.4.1 Rotation Anemometers

Until about 5–10 years ago, cup and propeller anemometers were the most common sensors used to measure wind speed. The cups used in anemometers have a round or preferably conical form, while the propellers have a helicoidal form that ensures a near-cosine response. Both systems consist of two parts: the rotor and the signal generator.

However, rotation anemometers are gradually being replaced by sonic anemometers, which can measure the wind vector with high accuracy and less maintenance than required for rotation anemometers. Classified cup anemometers are still used in the wind energy industry [9.57]. Cup anemometers positioned on high towers can perform measurements in the presence of inclination, acceleration, and vibration.

Handheld cup anemometers are also available. These have dynamo or mechanical counters; the lat-



**Fig. 9.12** Cup anemometer (photo © Th. Friedrichs & Co., Schenefeld, Germany)

ter give the windway, which can be recalculated into a wind speed within a certain time interval. Impeller wheel cup anemometers can also be obtained. While cup anemometers (Fig. 9.12) have distance constants of 2–5 m, those of propeller anemometers are on the order of 1–2 m. The latter are also able to measure turbulent fluctuations of up to 1–5 Hz and are available as three-component systems that can determine the wind vector (Fig. 9.13). An overview of different signal generators is given in Table 9.8.

Cup anemometers intended for application in moist and cold ( $< 0^{\circ}\text{C}$ ) weather conditions can be heated. The main components of the anemometer that are heated are the cups, the axis, and the bearings.

### 9.4.2 Wind Vanes

Wind vanes (Fig. 9.14) must be well balanced or they will adopt a preferred position at low wind speeds. When using mechanical anemometers, the wind direction can be determined using optical, electrical



**Fig. 9.13** The Gill 27005T UVW three-component propeller anemometer (photo © R.M. Young Company/GWU-Umwelttechnik GmbH, Erfstadt, Germany)

**Table 9.8** Overview of the signal generators used in cup and propeller anemometers [9.3]

Transducer	Outputs <sup>a</sup>	Power supply required?	Special features
<b>Cup anemometer</b>			
Current generator	AS (mA)	No	Manual anemometer
Contact transmitter with or without a counter	FS (Hz)	No	Selectable contact output sequence (manual anemometer)
Pulse generator (magnetic or inductive)	FS (Hz)	Yes	Not dependent on line resistances, linear output signal (standard signal)
Pulse generator (optoelectronic)	FS (Hz)	Yes	
Pulse generator with integrated signal converter	SS (mA, V)	Yes	
<b>Propeller anemometer</b>			
Optical pulse generator	FS (Hz)	Yes	Suitable for fluctuation measurements

<sup>a</sup> FS frequency signal (in Hz); AS scaled but often not linearized analog signal (resistance, voltage, or current); SS linearized standard signal, e.g., 0–20 mA, 4–20 mA or 0–5 V, 0–10 V

**Fig. 9.14** Mechanical wind vane (photo © Adolf Thies GmbH & Co. KG, Göttingen, Germany)

(potentiometer), or coding methods, as shown in Table 9.9. Potentiometers either have a dead zone near  $360^\circ$  or are  $540^\circ$  multiturn potentiometers. Similar to cup anemometers, heated wind vanes can be obtained for moist and cold weather conditions.

### 9.4.3 Combinations of a Rotation Anemometer with a Wind Vane

Various designs of systems combining a rotation anemometer with a wind vane are available. The cup anemometer may be separated from the wind vane vertically or horizontally (Fig. 9.15). In the case of horizontal separation, a large distance of about 1.0 to 1.5 m may be used to minimize interactions. When they are separated vertically, the lower of the two sensors may be affected by the mounting brackets.

A widely used sensor is the combination of a wind vane and a propeller anemometer (skyvane, Fig. 9.16). When there are large fluctuations in the wind direction, the wind speed measurement may be reduced due to the cosine response (see Sect. 9.3.1). Furthermore, the wind speed and the wind direction can be calculated from propeller anemometers with 2-D or 3-D designs (Fig. 9.13). An overview of different signal generators is given in Table 9.10.

### 9.4.4 Sonic Anemometers

Early sonic anemometers had a three-dimensional design, and their measurement paths were predominantly Cartesian oriented [9.27]. They were mainly applied for flux measurements (see Chap. 55). Modern sonic anemometers have larger measurement path angles to reduce flow distortion. Technical progress in the last 10–20 years has reduced the cost of a sonic anemometer dramatically, and this measuring principle is now also available for two-dimensional sensors that measure wind speed and direction. These sensors—which have a relatively open or compact design (Fig. 9.17)—are replacing rotating anemometers and wind vanes,

**Table 9.9** Overview of the signal generators used in mechanical wind vanes [9.3]

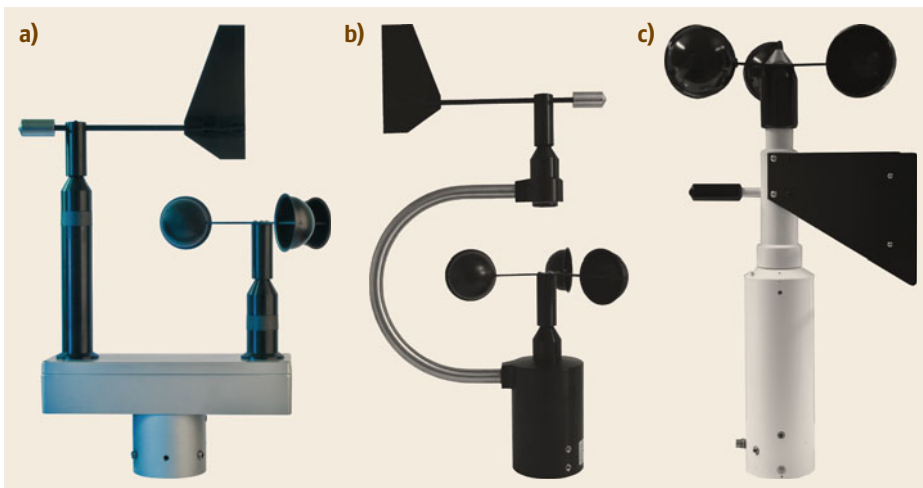
Transducer	Outputs <sup>a</sup>	Power supply required?	Special features
Potentiometer	AS ( $\Omega$ )	Yes	Very suitable for simple recorders/displays
Absolute angle encoder	GC, DP (serial or parallel)	Yes	Usually very expensive, encoding depends on manufacturer
(Optoelectronic) encoder	GC, DP (serial)	Yes	Standard, Gray code depends on manufacturer
Encoder with integrated signal converter	SS (mA, V)	Yes	Linear output signal (standard signal)

<sup>a</sup> AS scaled but often not linearized analog signal as resistance, voltage, or current signal; DP data protocols, e.g., via RS-232/485, SDI/MODBUS; GC Gray code: serial or parallel; SS linearized standard signal, e.g., 0–20 mA, 4–20 mA or 0–5 V, 0–10 V

**Table 9.10** Overview of the signal generators used in combinations of a rotation anemometer with a mechanical wind vanexo [9.3]

Devices combined	Transducer	Outputs <sup>a</sup>	Power supply required?	Special features
Cup anemometer combined with wind vane: vertical arrangement (coaxial)	Electric; see Tables 9.8 and 9.9		Yes	Compact design
Cup anemometer combined with wind vane: horizontal arrangement	Electric; see Tables 9.8 and 9.9		Yes	Large separation between the sensing devices
Wind vane with integrated propeller anemometer	Electric	FS (Hz), GC	Yes	
2-D (3-D) orthogonal propeller anemometer	Optical pulse generator	FS (Hz)	Yes	Suitable for fluctuation measurements

<sup>a</sup> FS frequency signal (in Hz); GC Gray code: serial or parallel

**Fig. 9.15a–c** Three combined system designs consisting of a cup anemometer and mechanical wind vane: (a) horizontally separated system (note: the distance between the sensors should be increased), (b) vertically separated system, (c) vertically separated system intended for application on ships (photo © Lambrecht Meteo GmbH, Göttingen, Germany)

even those used by meteorological services. They are available from many manufacturers and often included in complex weather sensors (see Chap. 43). Even one-dimensional sensors have become available; these

are used for measurements in a one-dimensional flow (Fig. 9.17c, industry) or in a combination of three sensors, such as in the wind turbine spinner [9.58] (see also Chap. 51).



**Fig. 9.16** Combination of a propeller anemometer with a mechanical wind vane, also called a skyvane (photo © R.M. Young Company/GWU-Umwelttechnik GmbH, Erfstadt, Germany)

An increasing number of designs and signal processing methods are becoming available for eddy covariance measurements. Figure 9.18 illustrates four different sensor types that are widely used. The DA700 (Fig. 9.18a) is the most recent version of the Kaijo-Denki PAT and DAT series of sensors that were used from the 1970s to 1990s in many scientific papers and are described in [9.22, 27]. The CSAT3 (Fig. 9.18b) is based on a prototype constructed at the University of

Washington [9.29], and has been used since the 1990s for scientific measurements. Both of these types are applied to a selected wind direction sector. If there is no preferred wind direction, omnidirectional anemometers are employed; two such sensors are shown in Fig. 9.18c, d. Further details on these sensors are given in Chap. 55.

Due to various issues with eddy covariance measurements, efforts have been made to reduce flow distortion by, for example, using smaller transducers or including a vertically oriented path that permits better resolution of the vertical wind velocity, even in omnidirectional sensors. Similar results of the reduction of the flow distortion are possible analyzing the signals between all transducers and not only along one path and the non-disturbed signals can be selected for the analysis. These investigations are ongoing, because wind tunnel measurements cannot be easily transferred to the turbulent atmosphere above various rough surfaces. Numerical studies are also used to improve anemometer design [9.59].

It is possible to heat a sonic anemometer in moist and frosty weather conditions, but this may influence the data [9.60, 61]. Because of the energy used in the transducers, a thin rough-frost layer does not significantly affect the measurements.

The wind data obtained using a sonic anemometer do not depend on the air density, but the power of



**Fig. 9.17** (a,b) Two-dimensional sonic anemometers with open path lengths; the latter has a compact construction (photos © Adolf Thies GmbH & Co. KG, Göttingen, Germany). (c) One-dimensional sonic anemometer (photo © METEK GmbH, Elmshorn, Germany)

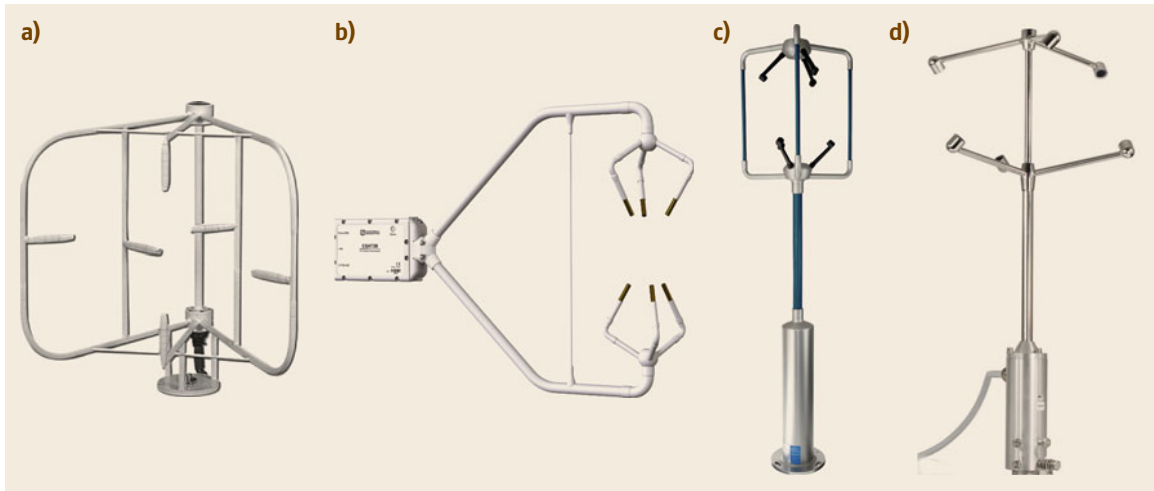


**Fig. 9.18a–d** Different types of three-dimensional sonic anemometers (the anemometers in (a) and (b) are orientated in one wind direction and those in (c) and (d) are omnidirectional types): (a) DA700 (photo © Sonic Corp., Tokyo, Japan), (b) CSAT3B (photo © Campbell Sci. Inc., Logan, UT, USA), (c) R3-50 (photo © Gill Instruments Ltd., Lymington, UK), and (d) uSonic-3 Scientific (formerly USA-1, photo © METEK GmbH, Elmshorn, Germany)

the sound transferred is density dependent. Most instruments have enough power to enable measurements to be performed at altitudes of up to about 5000 m, but the manufacturer should be consulted before performing such measurements.

#### 9.4.5 Thermal Anemometers

Thermal anemometers are robust sensors that are often combined with other sensors (see Chap. 43). This type of sensor type can be used in rough conditions. An example is shown in Fig. 9.19. The signal is either analog or digital (serial output).

#### 9.4.6 Hot-Wire Anemometers

Hot-wire anemometers use a thin metal wire (tungsten is common) or a quartz fiber (e.g., 70  $\mu\text{m}$ ) with a thin metal coating (e.g., 0.5  $\mu\text{m}$  of nickel) a few millimeters in length that is mounted on two needle-shaped prongs. The application of a combination of three wires can allow 3-D wind-vector measurements (Fig. 9.20).

Hot-wire anemometers have extremely high frequency responses and fine spatial resolutions compared to other measurement methods. Since the wire is very thin and hot, it is very delicate, it can be contaminated by gases and particles, and it suffers from aging. These sensors are therefore mainly employed in detailed studies of turbulent flows, preferably in clean air (laboratories), or for short field campaigns. Hot-wire anemometers only work correctly when the wind velocity is significant (typically above  $0.2 \text{ m s}^{-1}$ ), but they can be used at transsonic and sonic speeds.



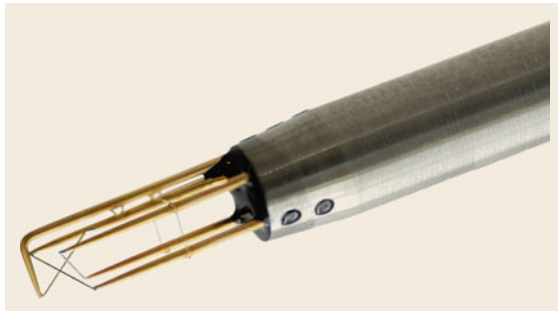
**Fig. 9.19** Thermal anemometer (top part) combined with a temperature screen (photo © Lambrecht Meteo GmbH, Göttingen, Germany)

#### 9.4.7 Laser Anemometers

The laser Doppler anemometer (LDA) has several advantages compared with most other techniques discussed in this chapter. First, due to their measurement principle, LDAs do not have to be calibrated! The observed Doppler shift is a linear function of the velocity component. However, the electronics needed to determine the Doppler shift is quite complex. Furthermore,

**Table 9.11** Advantages and disadvantages of different wind-measuring methods

Method or device	Advantages	Disadvantages
Cup anemometer	Simple and inexpensive anemometer, choice of many signal formats	Mechanical system, slow response time (large distance constant)
Propeller anemometer	Fast response time (low distance constant), but not good enough for turbulent flux measurements	Mechanically sensitive
Wind vane	Simple and inexpensive wind vane, choice of many signal formats	Mechanical system, slow response time (large distance constant)
Sonic anemometer	Nonmechanical device for measuring wind velocity and wind direction; fast response time, turbulence measurements are possible	Relatively expensive, special data calculations are necessary
Thermal anemometer	Nonmechanical device for measuring wind speed and wind direction	Low accuracy
Hot-wire anemometer	Very high wind velocities, very high resolution	Only for laboratory measurements, very sensitive mechanically
Laser anemometer	Fast-response anemometer	Only for laboratory measurements; requires the presence of a certain aerosol concentration
Pitot anemometer	Very robust, high wind velocities, high resolution	Requires high wind velocities, no wind direction (see multihole probe); beware of icing

**Fig. 9.20** Three-dimensional hot-wire anemometer (photo © Dantec Dynamics, Skovlunde, Denmark)

the measurement setup must be realized with high precision, and the angle  $\phi$  is almost linearly related to the wind component.

LDAs work very rapidly and offer very high temporal resolutions. Also, the measurement volume is extremely small—less than a millimeter in diameter. Since they have no moving parts, LDAs are low maintenance. They do not require contact with the medium and are unaffected by pressure, density, or temperature fluctuations in the flow.

## 9.5 Specifications

The general requirement for any wind-speed measuring device [9.4] is the ability to measure the wind speed up to  $75 \text{ m s}^{-1}$ . However, depending on the climate and measurement height (see Chap. 1), this range can be reduced for many sites. The required resolution and uncertainty depend on whether the application involves standard measurements or the measurement

of vertical gradients (which are commonly measured in research or for wind power studies). The typical requirements in both cases are given in Table 9.12. Requirements for standard wind direction measurements are given in Table 9.13. The specifications of the different types of wind sensors are given in Table 9.14.

### 9.4.8 Pitot-Static or Prandtl Tubes

However, LDAs are dependent on air particles. The final precision of the instrument also depends on the aerosol size distribution and concentration. LDAs are mainly applied in laboratories and wind tunnels; less often outdoors.

This method is mainly used at high velocities (e.g., aboard aircraft). A further development of the Prandtl tube is commonly used aboard research aircraft: the so-called multihole probe, which delivers not only the wind vector norm but all three components of the wind vector (see Chaps. 48 and 49).

### 9.4.9 Comparison of Different Methods

The appropriate wind sensor to use is determined by the measurement task. The essential aspects are the detection limit, resolution, dynamic behavior, measurement range, and either mechanical components or ultrasound. A comparison of the advantages and disadvantages of the various wind sensors described above is shown in Table 9.11.



**Table 9.12** Requirements for wind-speed sensing devices

Property	Standard use [9.3, 4]	Vertical gradients for flux calculations [9.3]
Range of wind speeds ( $\text{m s}^{-1}$ )	0–75	Dependent on measurement height
Distance constant (m)	2–5	$\leq 3$
Response threshold/detection limit ( $\text{m s}^{-1}$ )	$\leq 0.5$	$\leq 0.3$
Speed resolution ( $\text{m s}^{-1}$ )	$\pm 0.5$	$\pm 0.1$
Uncertainty	$\pm 0.5 \text{ m s}^{-1}$ for wind speeds $\leq 5 \text{ m s}^{-1}$ 10% for wind speeds $> 5 \text{ m s}^{-1}$	$\pm 0.1 \text{ m s}^{-1}$

**Table 9.13** Requirements for wind-direction sensing devices [9.3, 4]

Property	Wind vane	Ultrasound and thermal anemometers
Angular resolution (degrees)	5 for wind speeds $\geq 1 \text{ m s}^{-1}$	3 for wind speeds $\geq 1 \text{ m s}^{-1}$
Damping ratio	$> 0.3$	
Uncertainty (degrees)	$\pm 5$ at $u \geq 1 \text{ m s}^{-1}$	3 for wind speeds $\geq 1 \text{ m s}^{-1}$

**Table 9.14** Specifications of different methods for measuring the wind velocity and direction (given the large number of sensors available, the manufacturer's information should be used to retrieve more specific information on a particular sensor)

Sensor type	Typical uncertainty	Temperature range ( $^{\circ}\text{C}$ )	Remark
Cup anemometer	$\pm 0.3 \text{ m s}^{-1}$	$-40$ to $+70^{\text{a}}$	
Propeller anemometer (sky vane)	$\pm 0.1 \text{ m s}^{-1}$	$-40$ to $+60^{\text{b}}$	$0-35 \text{ m s}^{-1}$
Sonic anemometer	$\pm 0.1 \text{ m s}^{-1}, \pm 2^{\circ}$	$-40$ to $+70^{\text{a}}$	Resolution $0.01 \text{ m s}^{-1}$
Thermal anemometer	$\pm 0.5 \text{ m s}^{-1}, \pm 3^{\circ}$	$-40$ to $+70^{\text{a}}$	
Hot-wire anemometer	$\pm 0.01 \text{ m s}^{-1}$	$-20$ to $+70$	
Laser anemometer			
Pitot anemometer	0.5–5%	$-40$ to $+70^{\text{a}}$	
Wind vane	$\pm 5^{\circ}$	$-40$ to $+70^{\text{a}}$	

<sup>a</sup> When used at temperatures  $< 0^{\circ}\text{C}$  and in moist conditions, the sensor should be heated

<sup>b</sup> When used at temperatures  $< 0^{\circ}\text{C}$  and in moist conditions, the combined sensor and wind vane should be heated; otherwise, this combined system should only be used at temperatures above zero and in a dry climate

## 9.6 Quality Control

In contrast to other meteorological elements, the WMO [9.4] has not categorized standards for wind measurements. The ISO standards for wind tunnel calibration are applied to rotation and sonic anemometers [9.34, 41] (see Chap. 4), whereas cup anemometers for the wind energy industry are categorized by the International Electrotechnical Commission (IEC) [9.57]; see Chap. 51. A very general classification is used for sonic anemometers that are employed for flux measurements [9.62, 63]; see Table 9.15 and Chap. 55.

Anemometers are typically calibrated in wind tunnels. Because the calibrations are relatively stable over long periods, long time intervals can be left between calibrations (see Sect. 9.7) if the sensors are not mechanically deformed or corroded. However, wind tunnels provide near-laminar flow, and the characteristics in the turbulent atmosphere may be different to this.

This particularly applies to the flow distortion effects of sonic anemometers, which are usually reduced. For flux measurements performed using sonic anemometers, it is usual to carry out intercomparisons of different sensors. It is recommended that the instruments should not generate flow distortion effects for other sensors, the wind field should have the same turbulence characteristics for all sensors, and an instrument (etalon) for which the characteristics are already known should be used for comparison. For further aspects of such comparisons, see Chaps. 3 and 55.

### 9.6.1 Wind Tunnel Calibration

Rotation anemometers [9.34] must be calibrated in a wind tunnel to determine the linear transfer function (9.9), the nonlinear transfer function (9.10) (if they are

**Table 9.15** Classification of sonic anemometers based on the scheme given in [9.62, 63]

Anemometer class	Application	Sensor type
A	Flux measurements for basic research	3-D anemometer for flux measurements with an open sector of 120–300° when there are no significant flow distortion influences, e.g. Fig. 9.18a,b
B	General use for flux measurements	3-D anemometer for omnidirectional flux measurements (0–360°) when there are flow distortion influences due to the mounting structures, e.g. Fig. 9.18c,d
C	General use for wind measurements	2-D anemometer used only for the wind speed and direction, e.g. Fig. 9.17a,b

to be used to measure low wind speeds), the distance constant (9.11), and the cosine response (9.12); see Sect. 9.3.1 on rotation anemometers. With the exception of the distance constant and the nonlinear transfer function, the same characteristics of other types of anemometers (e.g., sonic anemometers) can also be measured in a wind tunnel.

#### Requirements for the Wind Tunnel

The wind tunnel should be large enough that the anemometer and of all the constructions required for the calibration cover less than 5% of the cross-sectional

area of a closed wind tunnel or less than 10% of the cross-sectional area of an open wind tunnel (Fig. 9.21). The cross-sectional profile of the anemometer and the constructions needed for calibration should remain the same during the process of calibration. If the diameter of the wind tunnel is too small for the anemometer, it is possible to calibrate the anemometer through comparison with another well-calibrated reference anemometer of the same type.

The wind speed of the tunnel should range from  $0 \text{ m s}^{-1}$  up to 50% of the maximum wind speed that the anemometer will encounter [9.34]. The speed should be kept constant to within  $\pm 0.2 \text{ m s}^{-1}$ . It is necessary to monitor the speed of the wind tunnel with well-calibrated (by a certificated institute), sensitive anemometers such as a hot-wire anemometer (Sect. 9.4.6), laser anemometer (Sect. 9.4.7), or Pitot tube (Sect. 9.4.8). The wind speed in the area of the anemometer should be uniform to within  $\pm 1\%$ . For wind speeds above  $10 \text{ m s}^{-1}$ , the turbulence intensity (the standard deviation of the mean wind speed divided by the mean wind speed) should be less than 2%. The turbulence intensity can be measured with a hot-wire or laser anemometer.

When determining the response threshold and the distance constant, the air density in the air stream should not vary by more than 3%, and for application of the Pitot anemometer, temperature and air density are necessary. Therefore, these parameters, together with the humidity, should be documented during the calibration.

#### Performing the Calibration

The lowest calibration point is approximately double the response threshold speed [9.34]. Other calibration points are 10, 20, 30, 40, and 50% of the maximum wind speed that the anemometer will encounter. Before calibration, the wind speed in the tunnel should be in a steady state. The averaging interval employed during calibration is 30–100 s, or even longer for anemometers with impulse output. The calibration should be repeated three times. The linear transfer function can be analyzed using regression analysis (see Chap. 2). If the

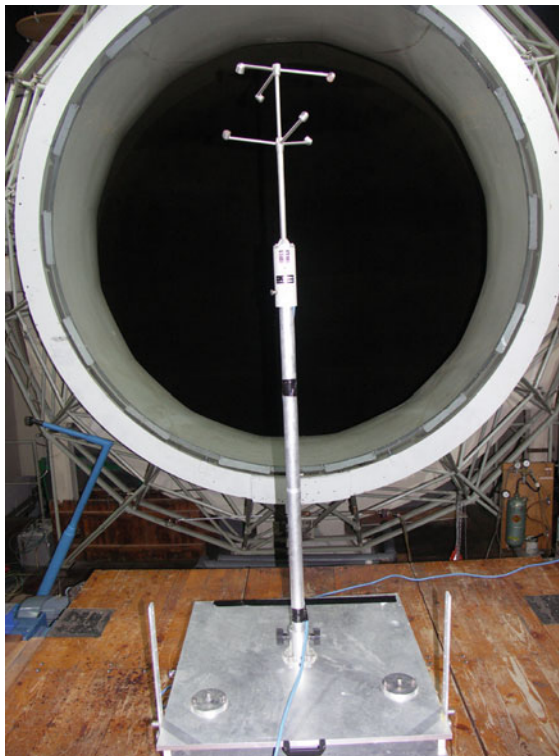


**Fig. 9.21** Wind tunnel calibration of a sonic anemometer in the low wind speed tunnel of the Technical University Dresden, Germany (photo © L. Siebicke)

relationship between the tunnel speed and the number of rotations or speed of the anemometer is not linear at lower wind speeds (Fig. 9.1), these wind speeds must be excluded from the linear transfer function and analyzed with (9.9), probably with the aid of more calibration points.

The determination of the distance constant should be repeated ten times for tunnel speeds of  $5 \text{ m s}^{-1}$  and  $10 \text{ m s}^{-1}$ . First the anemometer should be locked. After unlocking the anemometer, about ten measurements separated by time intervals that depend on the distance constant should be performed. The response time (see Chap. 2) is the time taken for the anemometer to change from 30 to 74% of the steady-state wind tunnel speed [9.34]. The distance constant is the average of all the measurements calculated with (9.11).

The cosine response calculated via (9.12) should be tested (with ten repetitions) for tunnel speeds of 5 and  $10 \text{ m s}^{-1}$ . To achieve this, the anemometer should be inclined in  $5^\circ$  steps up to  $30^\circ$  using a special construction. The cosine response of a cup anemometer should be negligible up to  $10\text{--}20^\circ$  [9.35]. Propeller and sonic anemometers should adhere closely to the cosine response; only small deviations are permissible for the propeller anemometer (Fig. 9.2). If necessary, the range of inclination can be extended to more than  $30^\circ$ .

### 9.6.2 Zero-Wind Chamber Calibration of Sonic Anemometers

The calibration of sonic anemometers is very stable for a long time. However, before the first use of the anemometer, a zero-point test should be carried out in a closed zero-wind chamber [9.41]. The size of the chamber required depends on the signal power of the anemometer and should be available from the manufacturer. Measurements of the wind components or wind speed in the chamber should be averaged over the same time interval as during the planned measurements. If the value is below the threshold of approximately  $0.01\text{--}0.1 \text{ m s}^{-1}$ , the test is complete. If not, there should be a check to see whether the test failed due to air flow in the chamber or signal reflection at the walls. If it did fail for either of these reasons, the position of the anemometer in the chamber should be changed. If the test fails again, the anemometer must be recalibrated by the manufacturer.

### 9.6.3 Specific Quality Control Methods

The following unrealistic values caused by a sensor malfunction or faulty data transmission during standard wind measurements should be identified through default testing and excluded [9.3, 64]:

- Negative values
- Wind speeds below the response threshold with a wind direction of  $1^\circ$  to  $360^\circ$
- Wind speeds above the response threshold with a wind direction of  $0^\circ$
- Wind speeds  $> 60 \text{ m s}^{-1}$  at elevations  $< 600 \text{ m}$  above mean sea level in Central Europe
- Wind speeds  $> 80 \text{ m s}^{-1}$  at elevations  $> 600 \text{ m}$  above mean sea level in Central Europe
- Wind direction  $> 360^\circ$
- A constant wind speed and/or direction for at least six hours.

Meteorological measurements can be tested by comparisons with climatological values regarding the variability of the wind speed and wind direction between two readings, or comparisons with wind measurements of nearby meteorological stations if they are not affected by their surroundings. This allows jumps in the readings (e.g., due to increased friction in the bearings) to be identified. Furthermore, the persistence of constant readings can be checked in order to identify blockages in the sensing device or a failed connection between the sensing device and data processing. The limit values are usually determined based on the typical measurements at the site.

Wind measurements taken at several sites or several altitudes can be tested by comparison with other data. The usual method is to identify measurement errors from a numerical analysis of weather reports for an extended area. The measurement of vertical gradients in the atmosphere near the ground can be checked by applying the typical logarithmic profile and obtaining approximate exponential profiles from tower measurements (see Chap. 1).

The abovementioned test can be performed not only for rotation anemometers but analogously for sonic and thermal anemometers. However, the measurement of standard deviations of wind variables or turbulent fluxes requires more comprehensive testing (see Chap. 55).

## 9.7 Maintenance

There are some general maintenance rules that should be followed for all wind-measuring instruments [9.3, 4]. The installed measuring system must be included in all maintenance actions (see Chap. 6). This includes the safety standards for masts, attachments, the fitting of a lightning conductor (on the upwind side of the anemometer), and meteorological requirements for the site, such as an undisturbed inflow direction (see Sect. 9.3.9).

Because wind sensors—especially mechanical sensors—are highly affected by environmental conditions, the following issues should be addressed during the maintenance:

- Lubricant viscosity and bearing properties are affected by aging and changes in temperature. Friction increases at low temperatures, which leads to erroneous measurement data. The manufacturers' instructions regarding temperature-related behavior must be observed.
- All wind-measuring instruments are subject to corrosion, especially when they are used in regions with high levels of air pollution, in coastal regions, or at sea. Corrosion effects should be identified and repaired.
- Appropriate measures should be put in place to ensure that birds cannot settle on the measuring instruments. A slightly higher mast close to and downwind of the tower can be helpful.

- Rain and snow can affect the properties of the equipment. In particular rime, hoar frost, and ice formation can completely interrupt the proper functioning of the measuring instrument unless these effects can be minimized (e.g., by heating).

For some sites, special actions are necessary, or the interval between maintenance should be shortened.

The calibration, inspection, and audit intervals of the sensing device and the data transmission and processing systems should be defined based on the required and specified accuracy and temporal changes, as should the interval between calibrations of electrical modules (which may present drift). Additional audits are necessary when the weather conditions (e.g., storms or snowfall) could affect the measurement process and/or the results obtained. Table 9.16 lists the maximum intervals between audits for standard meteorological measurements.

If regular weekly audits (see Table 9.16) of the equipment and the results of quality control (Sect. 9.6) indicate that the measuring and recording equipment is malfunctioning, immediate and more extensive inspections are necessary, as described in the other rows of Table 9.16. If the cause cannot be identified and remedied, the sensor should be replaced.

**Table 9.16** Maintenance of wind-measuring systems (updated from [9.3])

Maximum interval	Wind direction (wind vane)	Wind speed (rotation anemometer) <sup>a</sup>	Wind velocity and direction (sonic anemometer)
One week	Time control for digital recordings (time correction where required) Inspection of the data transmission Approximate review of the readings		
Six months	Inspection of the equipment carrier, including the sensing device and its mounting Inspection of the ambient conditions		
		Comparison of the measuring instrument with the reference instrument	
Two years	Inspection of the positioning Sensor calibration		Inspection of the zero-point drift [9.41]
If a check indicates that there is a possible malfunction, the instrument should be replaced			
<sup>a</sup> Similar actions for thermal anemometers			

## 9.8 Application

Wind data are widely used in science, weather prediction, the economy, and technical applications. From an economic perspective, wind climatology is useful for mitigating the damage caused by storm events, and for providing specific forecasts for wind power stations (see Chap. 51). Several technical processes are controlled by wind measurements, such as indoor climate control. All of these examples require precise standard measurements by meteorological stations and/or specific measurements performed near the objects of interest. For many purposes like wind power, building, and construction industry, special recommendations from international and national organizations are available.

Part E of this handbook discusses several methods that require wind data as input. Table 9.17 provides an overview of these methods and the wind measurements they require.

### 9.8.1 Climatology of Wind Parameters

As mentioned above, mean values of wind speed and direction over climatological periods of weeks, months, and up to 30-year periods are often meaningless, especially for the wind direction. The mean wind speed and its deviation from the long-term average are used to classify the availability of wind energy for wind power applications (see Chap. 51) during a particular period. Probability graphs that show the frequency distributions of different wind speed and wind direction classes (as

shown in Fig. 9.22) are much more useful. Such a graph allows the frequency of a certain wind speed or wind direction class to be determined for a potential application or site description. A frequency distribution such as that shown in Fig. 9.22b is also often presented in polar coordinates (a plot known as a *wind rose*, see Fig. 9.23a). Indeed, the wind-speed frequency distributions for particular wind-direction classes may be plotted in a similar manner (Fig. 9.23b). Such graphs can aid the interpretation of wind data for all wind-dependent processes. They are drawn for climatological periods (30 years) but should not be used for periods of less than ten years when attempting to characterize a site. Homogeneity of instrumentation and site conditions is required. For other purposes, shorter periods are possible.

### 9.8.2 Geostrophic Wind: Daily and Annual Cycles

The wind field is generated by differences in the amount of solar heat received by different regions of the Earth with the consequence of high- and low-pressure areas in the atmosphere that are significantly modified near the ground and by the rotation of the Earth. Above the atmospheric boundary layer (see Chap. 1), the wind is unaffected by the Earth's surface. This wind is called the geostrophic wind, and its speed can be calculated from the pressure gradients. For a positive Coriolis pa-

**Table 9.17** Wind data requirements for the measurement methods discussed in part E of this handbook (standard measurements are based on the WMO requirements [9.4])

Chapter no.	Chapter	Specific wind measurements
43	Weather Observation Stations for Different Purposes	Standard measurements
44	Crowdsourcing	All available measurements for crowdsourcing
45	Mesometeorological Networks	Standard and/or network-specific measurements
46	Aerological Measurements with Sondes	Standard measurements at the launch site
47	Vertical Composite Profiling	Standard measurements and vertical gradients at (high) towers
48	Aircraft-Based Measurements	Application of Pitot anemometers
49	Unmanned Aircraft System Measurements	Application of Pitot anemometers
50	Ground-Based Mobile Measurement Systems	Standard measurements and measurements on mobile platforms
51	Measurement Systems for Wind, Solar, and Hydro Power Applications	Standard measurements, vertical gradients at (high) towers, and measurements at wind power stations (spinners)
52	Urban Measurements and Interpretation	Standard measurements, vertical and horizontal gradients in complex terrain
54	Immision and Dry Deposition	Standard measurements, vertical gradients near the surface
55	Eddy-Covariance Measurements	Fluctuations of the wind vector and mean components
56	Alternative Surface Layer Flux Measurement Methods	Fluctuations of the wind vector and mean components
57	Evapotranspiration/Evaporation Measurements and Calculations	Standard measurements, vertical gradients near the surface, or fluctuations of the wind vector

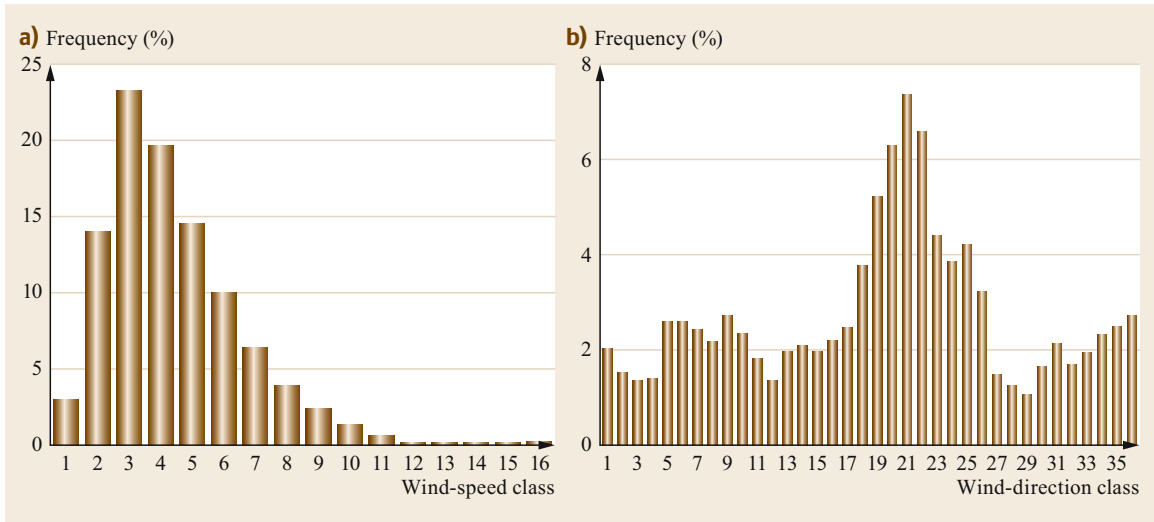


**Fig. 9.22a,b** Histograms showing typical frequency distributions for the wind speed (a) and the wind direction (b) (after [9.3] with permission from VDI e.V., Düsseldorf, Germany)

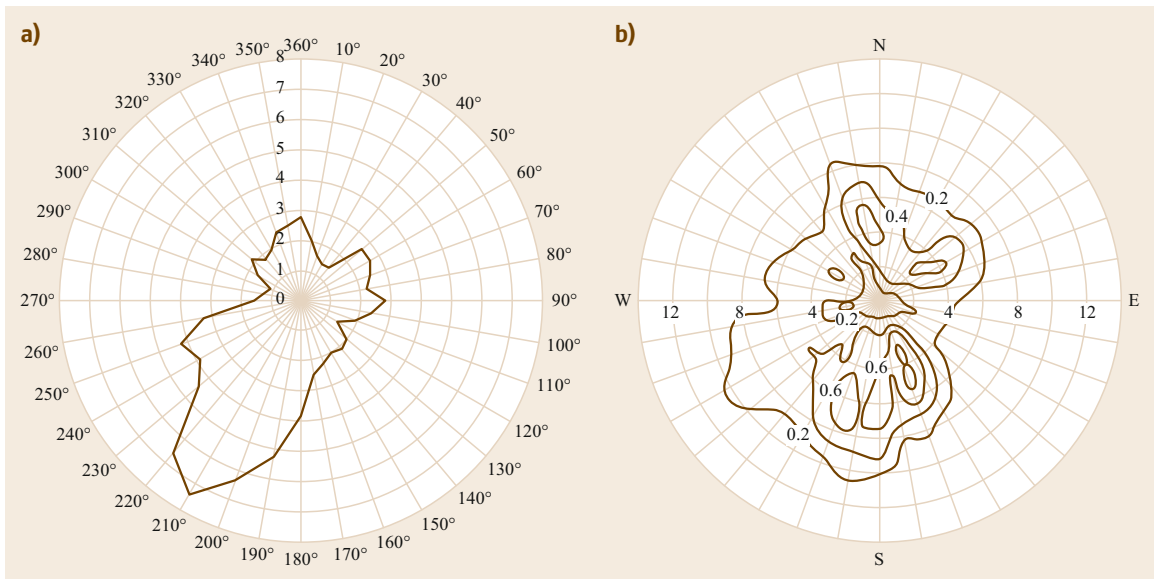


**Fig. 9.23a,b** Typical frequency distributions for the wind direction and wind speed plotted in polar coordinates (wind roses). Plot (a) shows the overall frequency distribution for the wind direction; the distance from the center of the plot is the relative frequency (in %) of the wind-direction class of interest. Plot (b) shows the frequency distribution (0.0–1.0) of the wind-speed as a function of the wind-direction class. Here, the distance from the center of the plot is the wind speed. In these plots, the wind direction and wind speed are split into classes  $10^\circ$  and  $1 \text{ m s}^{-1}$  wide, respectively (after [9.3] with permission from VDI e.V., Düsseldorf, Germany)



parameter  $f$ , the longitudinal component is

$$\overline{u}_g = -\frac{1}{\rho f} \frac{\partial p}{\partial y} \quad (9.43)$$

and the lateral component is

$$\overline{v}_g = \frac{1}{\rho f} \frac{\partial p}{\partial x}, \quad (9.44)$$

where  $\rho$  is the air density,  $p$  is the pressure, and

$$f = 2\Omega \sin \varphi, \quad (9.45)$$

in which  $\Omega$  is the angular velocity of the rotation of the Earth and  $\varphi$  is the geographical latitude. Geostrophic wind data can also be derived from pressure observations by meteorological stations and are available in databases.

Within the atmospheric boundary layer and near the ground, the wind speed typically exhibits a daily cycle with low wind speeds at night (when there is stable stratification of the atmosphere) and high wind speeds during the day (when there are unstable and convective conditions). The opposite cycle can be observed on a mountain above the nighttime inversion (see Chap. 1): at this altitude, the wind speed is not affected by the roughness of the Earth's surface, but the wind is slowed during the daytime by thermal processes that occur near to the surface of the mountain. Both of these daily cycles are illustrated in Fig. 9.24.

The annual cycle of the wind speed depends on the climate zone considered. In the temperate zone, high wind speeds are typically seen during transition times (spring and autumn) when low-pressure areas dominate. In other climate zones, wind systems such as trade winds, the monsoon, or even the hurricane season influence the annual cycle.

### 9.8.3 Gusts

Gusts are sudden, brief increases in the wind speed [9.65] that are barely affected by the surface

## 9.9 Future Developments

As also seen for other in-situ methods of obtaining atmospheric measurements, there has been a significant reduction in the variety of wind-measuring methods in recent decades. While hot-wire, laser, and Pitot anemometers are only applied for calibration purposes in laboratories, there has been an unmistakable shift from rotation anemometers to sonic anemome-

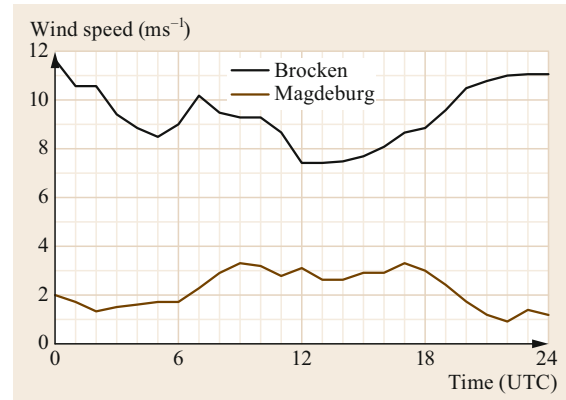


**Fig. 9.24** Daily cycle of the wind speed on Brocken, an isolated mountain (1142 m ASL) in Northern Germany, and the corresponding cycle about 75 km east of Brocken in the lowlands (Magdeburg, 76 m ASL) on 5 May 2018 during a high-pressure period (data from the DWD—the German Meteorological Service)

roughness or obstacles. Gusts are reported when the peak wind speed is larger than  $8 \text{ m s}^{-1}$ , the difference between the peak and the lulls is larger than  $4.5 \text{ m s}^{-1}$ , and the duration of the peak is less than 20 s. Because gusts can potentially cause damage, it is important to record them with anemometers, which requires a measurement range that reaches up to  $150 \text{ m s}^{-1}$  and an output averaging time of 3 s [9.4]. The sampling frequency should be about 4 Hz [9.66]. The recommended accuracy is only 10% [9.4]. Gusts are the main type of wind that can affect barometric readings [9.67] (see Chap. 10). The gustiness or turbulence intensity can be calculated; for example, for the longitudinal wind component [9.65],

$$g_u = \frac{\sqrt{u'^2}}{U}, \quad (9.46)$$

where  $U$  is the magnitude (modulus) of the wind vector. The other wind components and the horizontal wind speed are defined analogously.

ters. The number of sonic anemometers available has increased significantly over the last two decades. Specially designed devices that can perform flux measurements and analyze trace gases are available (see Chap. 55), and most manufacturers of meteorological instruments offer 2-D sonic anemometers as individual devices or within compact combined instruments (see

Chap. 43). Thermal anemometers are not an alternative to sonic anemometers and are only used for a few special purposes. Even meteorological services have replaced their rotation anemometers and wind vanes with sonic anemometers, albeit only with 2-D instruments (3-D instruments would offer more possibilities, including the ability to examine the stratification of the atmosphere). Only the wind power industry still recommends the use of rotation anemometers [9.57], and it has directed effort into increasing the accuracy of these instruments (see Chap. 51). Propeller

anemometers are only used in combination with wind vanes.

We can assume that this trend will continue, meaning that sonic anemometers will be the dominant devices used to measure the wind in-situ. Improving flow distortion correction (mainly the transducer correction; see Chap. 55) and facilitating multiple data analysis of all possible measurement paths will increase data accuracy and availability. Furthermore, sensor heating is easier to achieve for sonic anemometers than for rotation anemometers.

## 9.10 Further Reading

- VDI: Umweltmeteorologie, Meteorologische Messungen, Wind (Environmental Meteorology, Meteorological Measurements, Wind, in German and English), VDI 3786 Blatt(Part) 2, (Beuth-Verlag, Berlin 2018)
- WMO: Guide to Instruments and Methods of Observation, WMO-No. 8, Volume I - Measurement of Meteorological Variables. (World Meteorological Organization, Geneva, 2018)
- G. R. Harrison: Meteorological Measurements and Instrumentations, (John Wiley and Sons, Chichester 2015)
- F. V. Brock, S. J. Richardson: Meteorological Measurement Systems, (Oxford University Press, New York 2001)

**Acknowledgments.** We acknowledge several companies for allowing the reproduction of the photographs included in this chapter.

## References

- 9.1 J.C. Wyngaard: *Turbulence in the Atmosphere* (Cambridge Univ. Press, Cambridge 2010)
- 9.2 T. Foken: *Micrometeorology*, 2nd edn. (Springer, Berlin, Heidelberg 2017)
- 9.3 VDI: *Umweltmeteorologie, Meteorologische Messungen, Wind (Environmental Meteorology, Meteorological Measurements, Wind)*, VDI 3786, Blatt (Part) 2 (Beuth, Berlin 2018)
- 9.4 WMO: *Guide to Instruments and Methods of Observation*, WMO-No. 8, Volume I, Measurement of Meteorological Variables (WMO, Geneva 2018)
- 9.5 G. Hellmann: The dawn of meteorology, Q. J. R. Meteorol. Soc. **34**, 221–232 (1908)
- 9.6 W.E.K. Middleton: *Invention of the Meteorological Instruments* (The Johns Hopkins Press, Baltimore 1969)
- 9.7 E. Kleinschmidt (Ed.): *Handbuch der meteorologischen Instrumente und ihrer Auswertung* (Springer, Berlin 1935)
- 9.8 H.-G. Körber: *Vom Wetteraberglauben zur Wetterforschung* (Edition Leipzig, Leipzig 1987)
- 9.9 M. Centofanti: Egnazio Danti (1536–1586). In: *Distinguished Figures in Descriptive Geometry and Its Applications for Mechanism Science: From the Middle Ages to the 17th Century*, ed. by M. Cigola (Springer, Cham 2016) pp. 129–152
- 9.10 E. Gold: Wind in Britain: The Dines anemometer and some notable records during the last 40 years, Q. J. R. Meteorol. Soc. **62**, 167–206 (1936)
- 9.11 C.G. Herrmann: *Mechanisch verbesserter Wind-, Regen und Trockenheitsbeobachter* (Crazische Buchhandlung, Freyberg and Annaberg 1789)
- 9.12 K. Kreil: *Entwurf eines meteorologischen Beobachtungs-Systems für die österreichische Monarchie mit 15 Tafeln* (Kaiserlich-königliche Hof- und Staatsdruckerei, Wien 1850), nebst einem Anhang enthaltend die Beschreibung der an der K. K. Sternwarte zu Prag aufgestellten Autographen-Instrumente: Windfahne, Winddruckmesser, Regen- und Schneemesser
- 9.13 W.H. Dines: A new form of velocity anemometer, Q. J. R. Meteorol. Soc. **13**, 218–223 (1887)
- 9.14 T.R. Robinson: Description of an improved anemometer for registering the direction of the wind, and the space which it traverses in given intervals of time, Trans. R. Ir. Acad. **22**, 155–178 (1849)
- 9.15 C. Abbe: *The Aims and Methods of Meteorological Work*, Vol. I (Johns Hopkins Press, Baltimore 1899)
- 9.16 R.M. Schotland: The measurement of wind velocity by sonic waves, J. Meteorol. **12**, 386–390 (1955)
- 9.17 E.W. Barrett, V.E. Suomi: Preliminary report on temperature measurement by sonic means, J. Meteorol. **6**, 273–276 (1949)
- 9.18 V.E. Suomi: Sonic anemometer – University of Wisconsin. In: *Exploring the Atmosphere's First Mile*, Vol. 1, ed. by H.H. Lettau, B. Davidson (Pergamon, London, New York 1957) pp. 256–266

- 9.19 H.H. Lettau, B. Davidson (Eds.): *Exploring the Atmosphere's First Mile*, Vol. 1 (Pergamon, London, New York 1957)
- 9.20 V.M. Bovscheverov, V.P. Voronov: Akustitscheskii fljuzer (Acoustic rotor), *Izv. Akad. Nauk SSSR Geofiz.* **6**, 882–885 (1960)
- 9.21 J.C. Kaimal, J.A. Businger: A continuous wave sonic anemometer–thermometer, *J. Climate Appl. Meteorol.* **2**, 156–164 (1963)
- 9.22 Y. Mitsuta: Sonic anemometer–thermometer for general use, *J. Meteorol. Soc. Jpn.* **44**, 12–24 (1966)
- 9.23 J.C. Kaimal, J.E. Gaynor, H.A. Zimmerman, G.A. Zimmerman: Minimizing flow distortion errors in a sonic anemometer, *Bound.–Layer Meteorol.* **53**, 103–115 (1990)
- 9.24 V.M. Bovscheverov, B.M. Kaprov, M.I. Morduchovic: O trechkomponentnom akusticeskom anemometr (About a three–component acoustic anemometer), *Izv. Akad. Nauk SSSR Fiz. Atmos. Okeana* **9**, 434–437 (1972)
- 9.25 G.S. Campbell, M.H. Unsworth: An inexpensive sonic anemometer for eddy correlation, *J. Appl. Meteorol.* **18**, 1072–1077 (1979)
- 9.26 P.A. Coppin, K.J. Taylor: A three–component sonic anemometer/thermometer system for general micrometeorological research, *Bound.–Layer Meteorol.* **27**, 27–42 (1983)
- 9.27 T. Hanafusa, T. Fujitana, Y. Kobori, Y. Mitsuta: A new type sonic anemometer–thermometer for field operation, *Papers Meteorol. Geophys.* **33**, 1–19 (1982)
- 9.28 J.C. Wyngaard: The effects of probe–induced flow distortion on atmospheric turbulence measurements, *J. Appl. Meteorol.* **20**, 784–794 (1981)
- 9.29 S.F. Zhang, J.C. Wyngaard, J.A. Businger, S.P. Oncley: Response characteristics of the U.W. sonic anemometer, *J. Atmos. Ocean. Technol.* **2**, 548–558 (1986)
- 9.30 T. Foken, R. Dlugi, G. Kramm: On the determination of dry deposition and emission of gaseous compounds at the biosphere–atmosphere interface, *Meteorol. Z.* **4**, 91–118 (1995)
- 9.31 H. Pitot: Description d'une machine pour mesurer la vitesse des eaux courantes et le sillage des vaisseaux. In: *Histoire de l'Académie royale des sciences avec les mémoires de mathématique et de physique tirés des registres de cette Académie*, ed. by Académie des sciences (Imprimerie Royale, Paris 1732) pp. 363–376
- 9.32 H. Darcy: Note relative à quelques modifications à introduire dans le tube de Pitot, *Ann. Ponts Chaussées Ser. 3* **1**, 351–359 (1858)
- 9.33 H. Herwig: *Strömungsmechanik: Einführung in die Physik von technischen Strömungen* (Springer, Berlin, Heidelberg 2016)
- 9.34 ISO 17713–1: *Meteorology – Wind Measurements – Part 1: Wind Tunnel Test Methods for Rotating Anemometer Performance* (Beuth, Berlin 2007)
- 9.35 F.V. Brock, S.J. Richardson: *Meteorological Measurement Systems* (Oxford Univ. Press, New York 2001)
- 9.36 L. Kristensen: Cup anemometer behavior in turbulent environments, *J. Atmos. Ocean. Technol.* **15**, 5–17 (1998)
- 9.37 R. Drinkov: A solution to the paired gill–anemometer response function, *J. Climate Appl. Meteorol.* **11**, 76–80 (1972)
- 9.38 T. Foken, H. Kaiser, W. Rettig: *Propelleranemometer: Überblick und spezielle Entwicklungen am Meteorologischen Hauptobservatorium Potsdam*, Veröffentlichungen des Meteorologischen Dienstes der Deutschen Demokratischen Republik, Vol. 24 (Adademie–Verlag, Berlin 1983)
- 9.39 A.J. Bowen, H.W. Teunissen: Correction factors for the directional response of gill propeller anemometer, *Bound.–Layer Meteorol.* **37**, 407–413 (1986)
- 9.40 J.C. Kaimal, J.J. Finnigan: *Atmospheric Boundary Layer Flows: Their Structure and Measurement* (Oxford Univ. Press, New York 1994)
- 9.41 ISO 16622: *Meteorology – Sonic Anemometer/Thermometer – Acceptance Test Method for Mean Wind Measurements* (Beuth, Berlin 2002)
- 9.42 H. Eckelmann: *Einführung in die Strömungsmesstechnik* (Teubner, Stuttgart 1997)
- 9.43 A.–E. Albrecht, M. Borys, N. Damaschke, C. Tropea: *Laser Doppler and Phase Doppler Measurement Techniques* (Springer, Berlin, Heidelberg 2003)
- 9.44 P.B. MacCready, H.R. Jex: Response characteristics and meteorological utilization of propeller and vane wind sensors, *J. Appl. Meteorol.* **3**, 182–193 (1964)
- 9.45 J. Wieringa: Evaluation and design of wind vanes, *J. Appl. Meteorol.* **6**, 1114–1122 (1967)
- 9.46 T.P. DeFelice: *An Introduction to Meteorological Instrumentation and Measurement* (Prentice Hall, Upper Saddle River 1998)
- 9.47 P.L. Finkelstein: Measuring the dynamic performance of wind vanes, *J. Appl. Meteorol.* **20**, 588–594 (1981)
- 9.48 ISO 19289:2015: *Air Quality – Meteorology – Siting Classifications for Surface Observing Stations on Land* (WMO, Geneva 2015)
- 9.49 A.G. Davenport, C.S.B. Grimmond, T.R. Oke, J. Wieringa: Estimating the roughness of cities and sheltered country. In: *Proc. 12th Conf. App. Climatol* (American Meteorological Society, Boston, MA 2000) pp. 96–99
- 9.50 J. Wieringa: Updating the Davenport roughness classification, *J. Wind Eng. Ind. Aerodyn.* **41**, 357–368 (1992)
- 9.51 I. Troen, E. Lundtang Peterson: *European Wind Atlas* (Risø National Laboratory, Roskilde 1989)
- 9.52 E.L. Mollo–Christensen, J.R. Seesholtz: Wind tunnel measurements of the wind disturbance field of a model of the Buzzards Bay entrance light tower, *J. Geophys. Res.* **72**, 3549–3556 (2012)
- 9.53 P.A. Taylor, R.J. Lee: Simple guidelines for estimating wind speed variations due to small scale topographic features, *Climatol. Bull.* **18**, 3–22 (1984)
- 9.54 J.L. Walmsley, I. Troen, D.P. Lalas, P.J. Mason: Surface–layer flow in complex terrain: comparison of models and full–scale observations, *Bound.–Layer Meteorol.* **52**, 259–281 (1990)
- 9.55 WMO: *Meteorological Aspects of the Utilization of Wind as an Energy Source*, Techn. Note 175 (WMO, Geneva 1981)

- 9.56 M.D. Perera: Shelter behind two dimensional solit and porous fences, *J. Wind Eng. Ind. Aerodyn.* **8**, 93–104 (1981)
- 9.57 IEC 61400-12-1: *Wind Energy Generation Systems – Part 12-1: Power Performance Measurements of Electricity Producing Wind Turbines*, 2017-03, 2nd edn. (VDE, Berlin 2017)
- 9.58 F.P. Troels, N.N. Sørensen, L. Vita, P. Enevoldsen: *Optimization of Wind Turbine Operation by Use of Spinner Anemometer*, Risø-Report No. 1654, 2008) p. 45
- 9.59 S. Huq, F. De Roo, T. Foken, M. Mauder: Evaluation of probe-induced flow distortion of campbell Csat3 sonic anemometers by numerical simulation, *Bound.-Layer Meteorol.* **165**, 9–28 (2017)
- 9.60 F. Kittler, W. Eugster, T. Foken, M. Heimann, O. Kolle, M. Göckede: High-quality eddy-covariance CO<sub>2</sub> budgets under cold climate conditions, *J. Geophys. Res. Biogeosci.* **122**, 2064–2084 (2017)
- 9.61 J.P. Goodrich, W.C. Oechel, B. Gioli, V. Moreaux, P.C. Murphy, G. Burba, D. Zona: Impact of different eddy covariance sensors, site set-up, and maintenance on the annual balance of CO<sub>2</sub> and CH<sub>4</sub> in the harsh arctic environment, *Agric. Forest Meteorol.* **228/229**, 239–251 (2016)
- 9.62 T. Foken, S.P. Oncley: Results of the workshop instrumental and methodical problems of land surface flux measurements, *Bull. Am. Meteorol. Soc.* **76**, 1191–1193 (1995)
- 9.63 M. Mauder, C. Liebenthal, M. Göckede, J.-P. Leps, F. Beyrich, T. Foken: Processing and quality control of flux data during LITFASS-2003, *Bound.-Layer Meteorol.* **121**, 67–88 (2006)
- 9.64 A.T. DeGaetano: A quality-control routine for hourly wind observations, *J. Atmos. Ocean. Technol.* **14**, 308–317 (1997)
- 9.65 T.S. Glickman (Ed.): *Glossary of Meteorology*, 2nd edn. (Am. Meteorol. Soc., Boston, MA 2000)
- 9.66 J. Wieringa: Representativeness of wind observations at airports, *Bull. Am. Meteorol. Soc.* **61**, 962–971 (1980)
- 9.67 H. Liu, G.L. Darkow: Wind effect on measured atmospheric pressure, *J. Atmos. Ocean. Technol.* **6**, 5–12 (1989)

### Thomas Foken

University of Bayreuth  
Bayreuth, Germany  
[thomas.foken@uni-bayreuth.de](mailto:thomas.foken@uni-bayreuth.de)



Thomas Foken is a retired Professor of Micrometeorology at the University of Bayreuth. He was the head of Laboratories at the meteorological observatories at Potsdam (1981–1994) and Lindenberg (1994–1997). His research interests include the interaction between the Earth's surface and the atmosphere and the measurement and modeling of energy and matter fluxes, with a strong focus on experimental meteorology. His scientific contributions have been recognized through various international awards.

### Jens Bange

Centre for Applied Geo-Science  
University of Tübingen  
Tübingen, Germany  
[jens.bange@uni-tuebingen.de](mailto:jens.bange@uni-tuebingen.de)



Jens Bange is a Professor for Environmental Physics at the University of Tübingen since 2010. He received a PhD in meteorology in 1998 and a diploma in physics in 1992 at the University of Hannover. His research interests include atmospheric turbulence, boundary-layer meteorology, wind-energy research, airborne meteorology, and environmental measurement technology. He is a founding member of the research networks ISARRA and WindForS.